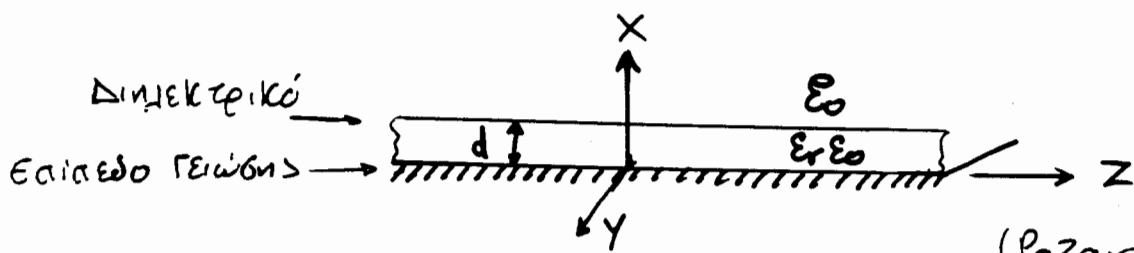


## **ΚΕΦΑΛΑΙΟ 2**

<b>Μικροκυματικά Στοιχεία – Τυπωμένες Γραμμές</b>	<b>Σελίδα</b>
• Επιφανειακά Κύματα σε Γειωμένο Διηλεκτρικό	2- 1
• Τυπωμένες – Ολοκληρωμένες Μικροταινιακές Γραμμές	2- 6
• Μικροκυματικοί Πυκνωτές και Πηνία	2-10
• Μομολιθικά Μικροκυματικά Στοιχεία MMIC's	2-12
• Τυπωμένοι Μικροκυματικοί Συζεύκτες	2-16
• Μικροκυματικά Τρανζίστορ MESFET, HEMT, HBT	2-17

# ΕΠΙΦΑΝΕΙΑΚΑ ΚΥΜΑΤΑ ΣΕ ΓΕΙΟΜΕΝΟ ΔΙΗΛΕΚΤΡΙΚΟ



(Pozar GEJ. 170)

- Επιφανειακοί ρυθμοί διεγείρονται σε: μη-γειωμένη (και γειωμένη) διηλεκτρική πλάκα, διηλεκτρικό ρύθμο, αγγελή ρύθμο με διηλεκτρική επικαύση και

→ Τα Επιφανειακά κύματα χαρακτηρίζονται από την μεγάλη εποχή που διατηρείται προς το διηλεκτρικό (άφονα -x;  $e^{-\alpha x}$ ) και διάδοση παρατίνα με το αγγελή ρύθμο γειαστό.

- Όσο αυταρται η διανομή του περιβολεύοντος Η/Μ πεδίου περιορίζεται μέσα και κατά το διηλεκτρικό  $\Rightarrow$

$\Rightarrow$  Επιφανειακοί κύματα διδύμοις

(Τυπωμένες μικροκυκλωτικές γραμμές - Μικροσανίκες, τανινιογράφης κ.)

ΡΥΘΜΟΙ TM  $\rightarrow$  TM<sub>z</sub>  $\rightarrow$  H<sub>z</sub> = 0

ΥΠΟΔΕΙΓΜΑΤΑ: { Διαίσθοντας στην διεύθυνση -z  $\Rightarrow \bar{E}, \bar{H} \propto e^{j\beta z}$   
 { Αμεταβλητό πεδίο στην διεύθυνση -y  $\Rightarrow \frac{\partial}{\partial y} = 0$   
 (Η διαταγή εκρεινεται απεριόριστα στην διεύθυνση -y)

Η διανομή E<sub>z</sub> πρέπει στην επίσημη κύματος:

Περιοχή αέρα  $x \geq d$ :  $\bar{\nabla}_t^2 E_{z1} + k_0^2 E_{z1} = 0$  ①

Περιοχή διηλεκτρικού  $0 \leq x \leq d$ :  $\bar{\nabla}_t^2 E_{z2} + k_e^2 E_{z2} = 0$  ②

Όπου  $\bar{\nabla}_t^2 = \frac{\partial^2}{\partial x^2} + \frac{\partial^2}{\partial z^2}$  } Θεσμοί:  $E_z(x, y, z) = E_z(x, y) e^{j\beta z}$   
 $k_0^2 = \omega^2 \mu_0 \epsilon_0$        $k_e^2 = \omega^2 \mu \epsilon = \epsilon_r k_0^2$  } αριθμ.:  $\bar{\nabla}_t^2 E_z = \frac{\partial^2 E_z}{\partial x^2} + (-j\beta)^2 E_z$

$$\textcircled{1} \rightarrow \frac{\partial^2 E_{z1}(x, y)}{\partial x^2} + \overbrace{(k_0^2 - \beta^2)}^{\rightarrow -h} E_{z1}(x, y) = 0 \quad j/a \quad x \geq d$$

$$\textcircled{2} \rightarrow \frac{\partial^2 E_{z2}(x, y)}{\partial x^2} + \overbrace{(\epsilon_r k_0^2 - \beta^2)}^{+K_e^2} E_{z2}(x, y) = 0 \quad j/a \quad 0 \leq x \leq d$$

Q=1

ΡΥΘΜΟΙ ΤΜ  $\leftrightarrow$  ΕΠΙΦΑΝΕΙΑΚΗ ΚΥΦΑΣA  $H_z = 0$

Λιγη ΣΦΙΓΩΣΕΙΝ ΚΥΦΑΣΑ:

$$\text{Περιοχή αέρα} \quad E_{z1}(x,y) = C e^{hx} + D e^{-hx} \quad x \geq d \quad (3)$$

$$-\text{Διηγεικρική} \quad E_{z2}(x,y) = A \sin(K_e x) + B \cos(K_e x) \quad 0 \leq x \leq c$$

Οριακές Συνθήσεις: οπου  $h^2 = -(K_0^2 - \beta^2)$  και  $K_e^2 = (\epsilon_r K_0^2 - \beta^2)$  (4)

a) Μηδενικός των Εραπλούντικων  $H_z$  στην περιοχή  $x > d$  γειωμένο αριώγιμο όριο:  $E_{z2}|_{x=0} = 0 : (4) \rightarrow B = 0$

b) Οριακή δυνατή ακτινοβολίας

$E_{z1}|_{x \sim \infty} \rightarrow$  πεπερασμένο πεδίο και αεπερασμένη ενέργεια μεταξύ αυτού την πηγή  $\rightarrow C = 0$

c) Συνέχεια των Εραπλούντικων ηλεκτρικών πεδίων στην οριακή επιφάνεια αέρα - διηγεικρικής  $E_{z1}|_{x=d^+} = E_{z2}|_{x=d^-}$  και  $E_{y1}|_{x=d^+} = E_{y2}|_{x=d^-}$

$$\left. \begin{array}{l} E_{z1}(x,y) = D e^{-hx} \\ E_{z2}(x,y) = A \sin(K_e x) \end{array} \right\} \begin{array}{l} \downarrow \\ A \sin(K_e d) = D e^{-hd} \end{array} \quad \frac{\partial}{\partial y} = 0 \rightarrow E_y = 0 \quad (5)$$

d) Συνέχεια των Εραπλούντικων μαγνητικών πεδίων ( $\bar{H}_t$ ) στην οριακή επιφάνεια αέρα - διηγεικρικής:

$$\bar{H}_t = H_y \hat{y} + H_z \hat{z} \implies H_{y1}|_{x=d^+} = H_{y2}|_{x=d^-}$$

$$H_y = \frac{-j\omega \epsilon}{K_e^2} \frac{\partial E_z}{\partial x}$$

$$\frac{(-j\omega \epsilon)}{K_e^2} (-h) \cdot D e^{-hd} = \frac{(-j\omega \epsilon) \epsilon_r}{K_e^2} (A K_e) \cos(K_e d) \quad (6)$$

Κυματοποιητικοί αποκοντιστές:

$$\left. \begin{array}{l} h = j K_x, \beta = K_z, K_e = K_x z \\ K_e^2 = K_x^2 + K_y^2 \\ K_e^2 + K_z^2 = K^2 \end{array} \right\} \begin{array}{l} K_{c1}^2 = K_0^2 - \beta^2 = -h^2 \leftrightarrow h^2 = \beta^2 - K_0^2 \\ K_{c2}^2 = K^2 - \beta^2 = K_e^2 \rightarrow K_e^2 = (\beta^2 - \epsilon_r K_0^2) \end{array}$$

$$(5) \rightarrow A \sin(K_e d) = D e^{-hd} \quad \left\{ \begin{array}{l} K_e \tan(K_e d) = +\epsilon_r h \end{array} \right.$$

$$(6) \rightarrow \frac{\epsilon_r A}{K_e} \cos(K_e d) = +\frac{D}{h} e^{-hd} \quad \left\{ \begin{array}{l} K_e \tan(K_e d) = +\epsilon_r h \end{array} \right.$$

$$\left( \text{Shannus} \right) \left\{ \begin{array}{l} \frac{d^2 y}{dx^2} + b y = 0 \\ y = C_1 \cos(qx) + C_2 \sin(qx) \end{array} \right. \rightarrow \left\{ \begin{array}{l} y = C_1 e^{m_1 x} + C_2 e^{m_2 x} \quad \text{οπου } m_{1,2}^2 = -b \\ q^2 = +b \end{array} \right.$$

ΠΥΘΜΟΙ ΤΕ  $\leftrightarrow$  ΕΠΙΦΑΝΕΙΑΛΟΥ Κύματος  $E_2 = 0, H_2 \neq 0$

Εφιγωγή Κύματος με  $\frac{\partial}{\partial z} = -j\beta$  και  $\frac{\partial}{\partial y} = 0, H_2 = h_{21}(x,y) e^{j\phi}$

$$\text{Τέτοια ως: } \bar{V}_E^2 H_{21} + K_0^2 H_{21} = 0 \leftrightarrow \frac{\partial^2 h_{21}(x,y)}{\partial x^2} + (K_0^2 - \beta^2) h_{21}(x,y) = 0$$

$$\text{Τέτοια όρια: } \bar{V}_E^2 H_{22} + K_0^2 H_{22} = 0 \leftrightarrow \frac{\partial^2 h_{22}(x,y)}{\partial x^2} + (K_0^2 - \beta^2) h_{22}(x,y) = 0$$

Λύσεις:

$$\text{Πρώτη αίρα: } h_{21}(x,y) = C e^{hx} + D e^{-hx} \quad \text{για } x \geq d$$

$$\text{-η- συνήθεια: } h_{22}(x,y) = A \sin(K_m x) + B \cos(K_m x) \quad 0 \leq x \leq d$$

$$\text{όπου } -h^2 = K_0^2 - \beta^2 = K_1^2, K_m^2 = \varepsilon_r K_0^2 - \beta^2 = K_{c2}$$

Οριακές Συνθήκες:

a) Μηδενικός Εξαπολεμένου Ηλεκτρ. Πεδίου γειωμένο αγ. εσ.

$$E_{y2} = -\frac{j\omega\mu}{K_{c2}} \frac{\partial H_{22}}{\partial x} \Big|_{x=0} = 0 \rightarrow \frac{\partial h_{22}}{\partial x} \Big|_{x=0} = K_m [A \cos(K_m x) - B \sin(K_m x)] = 0$$

$$\rightarrow \underline{A=0} \quad \text{και} \quad h_{22}(x,y) = B \cos(K_m x)$$

b) Οριακή Γωνία λατ. νορθοβολίας

$$H_{21} \Big|_{x \approx d} \sim \text{ΠΕΠΕΡΑΣΜΕΝΟ} \rightarrow C=0 \quad \text{και} \quad h_{21}(x,y) = D e^{-hx}$$

c) Συνέχεια των Εφαπτομένων Ηλεκτρ. Πεδίων σε όποιο αέρα - διηγέτηρικοι

$$E_{y1} \Big|_{x=d^+} = E_{y2} \Big|_{x=d^-} \rightarrow \frac{-j\omega\mu_0}{K_{c1}} e^{j\beta x} \frac{\partial h_{21}}{\partial x} \Big|_{x=d^+} = \frac{-j\omega\mu_0}{K_{c2}} e^{j\beta x} \frac{\partial h_{22}}{\partial x} \Big|_{x=d^-} \\ \rightarrow \frac{\mu_0}{(-h^2)} (-K) \cdot D e^{-hd} = \frac{\mu_0}{K_m^2} (-K_m) B \sin(K_m d) \quad \textcircled{1}$$

d) Συνέχεια των Εφαπτομένων Μαγν. Πεδίων σε όποιο αέρα - διηγέτηρικοι

$$\bar{H}_E = H_y \hat{y} + H_z \hat{z} \quad \text{αλλα} \quad H_y = -j\beta \frac{\partial H_z}{\partial y} \quad \text{με} \quad \frac{\partial}{\partial y} = 0 \rightarrow H_y = 0$$

$$H_{21} \Big|_{x=d^-} = H_{22} \Big|_{x=d^+} \rightarrow h_{21} \Big|_{x=d^-} = h_{22} \Big|_{x=d^+} \rightarrow D e^{-hd} = B \cos(K_m d)$$

$$\textcircled{1} \quad \frac{\mu_0}{h} D e^{-hd} = -\frac{\mu_0}{K_m} B \sin(K_m d) \quad \textcircled{2}$$

$$\textcircled{2} \quad D e^{-hd} = B \cos(K_m d) \quad \left\{ h = \frac{K_m}{\mu_0} \cot(K_m d) \Rightarrow K_m \cot(K_m d) = -h \right\}$$

# ΣΥΧΕΤΙΣΗ ΕΓΚΑΡΣΙΩΝ ΚΑΙ ΑΞΟΝΙΚΩΝ ΣΥΝΙΣΤΟΥΣΩΝ

- Διάδοση κατά λντρίδες - z :  $\bar{E}, \bar{H} \propto e^{-j\beta z} \rightarrow \frac{\partial}{\partial z} = -j\beta$
- Συνδιαίρετας της δύο εφιγώγεις γεφορίδας  
Για χωρό καρπίς πηγές  $\bar{J} = 0, \rho = 0$   
 $\bar{\nabla} \times \bar{E} = -j\omega \mu \bar{H}$        $\bar{\nabla} \times \bar{H} = j\omega \epsilon \bar{E}$

Πυρήναι  $TE \rightarrow TE_z$  :

$$E_z = 0, H_z \neq 0$$

$$E_x = -\frac{j\omega \mu}{k_c^2} \frac{\partial H_z}{\partial y}$$

$$E_y = \frac{j\omega \mu}{k_c^2} \frac{\partial H_z}{\partial x}$$

$$H_x = -\frac{j\beta}{k_c^2} \frac{\partial H_z}{\partial x}$$

$$H_y = -\frac{j\beta}{k_c^2} \frac{\partial H_z}{\partial y}$$

Πυρήναι  $TM \rightarrow TM_z$

$$H_z = 0, E_z \neq 0$$

$$E_x = -\frac{j\beta}{k_c^2} \frac{\partial E_z}{\partial x}$$

$$E_y = -\frac{j\beta}{k_c^2} \frac{\partial E_z}{\partial y}$$

$$H_x = \frac{j\omega \epsilon}{k_c^2} \frac{\partial E_z}{\partial y}$$

$$H_y = -\frac{j\omega \epsilon}{k_c^2} \frac{\partial E_z}{\partial x}$$

$$\text{Όπου } \beta = \sqrt{k^2 - k_c^2} \rightarrow k_c^2 = k^2 - \beta^2 \quad \text{και} \quad j \rightarrow j\beta \quad (\alpha \neq 0)$$

$$k_c^2 = k_x^2 + k_y^2, \quad k_c^2 + k_z^2 = k^2, \quad \beta = k_z$$

$$H_z = \begin{cases} D e^{-hx} e^{-j\beta z} & \text{αέρας} \\ B \cos(k_m x) e^{-j\beta z} & \text{διηλεκτ.} \end{cases}$$

$$E_z = \begin{cases} D e^{-hx} e^{-j\beta z} & \text{αέρας} \\ A \sin(k_m x) e^{-j\beta z} & \text{διηλεκτ.} \end{cases}$$

$$k_m \cot(k_m d) = -\mu_r h$$

$$D = B e^{hd} \cos(k_m d)$$

$$h^2 = \beta^2 - k_0^2 = -k_{c1}^2$$

$$k_m^2 = k^2 - \beta^2 = \epsilon_r \mu_r k_0^2 - \beta^2 = k_{c2}^2$$

$$\beta^2 = h^2 + k_c^2 = \epsilon_r \mu_r k_0^2 - k_m^2$$

$$h^2 + k_c^2 = k_0^2 (\epsilon_r \mu_r - 1)$$

$$k_e \tan(k_e d) = \epsilon_r h$$

$$D = A e^{hd} \sin(k_e d)$$

$$h^2 = \beta^2 - k_0^2 = -k_{c1}^2$$

$$k_e^2 = k^2 - \beta^2 = \epsilon_r \mu_r k_0^2 - \beta^2 = k_{c2}^2$$

$$\beta^2 = h^2 + k_c^2 = \epsilon_r \mu_r k_0^2 - k_e^2$$

$$h^2 + k_c^2 = k_0^2 (\epsilon_r \mu_r - 1)$$

H/M ΠΕΔΙΟ ΕΠΙΦΑΝΕΙΑΚΩΝ ΡΥΘΜΩΝ

ΡΥΘΜΟΙ TM

$$\begin{array}{l}
 \text{περιοχή ασφα } x \geq d \\
 E_2 = A \sin(k_e d) e^{-h(x-d)} e^{-j\beta z} \\
 E_x = -j\beta A \sin(k_e d) e^{-h(x-d)} e^{-j\beta z} \\
 E_y = 0, H_x = 0 \\
 H_y = -j\frac{\omega \epsilon_0}{h} A \sin(k_e d) e^{-h(x-d)} e^{-j\beta z} \\
 H_z = 0
 \end{array}
 \quad \left| \begin{array}{l}
 H_2 = B \cos(k_m d) e^{-h(x-d)} e^{-j\beta z} \\
 E_x = 0 \\
 E_y = j\frac{\omega \mu_0}{h} B \cos(k_m d) e^{-h(x-d)} e^{-j\beta z} \\
 E_2 = 0, H_y = 0 \\
 H_x = -j\frac{\beta}{h} B \cos(k_m d) e^{-h(x-d)} e^{-j\beta z}
 \end{array} \right.$$

περιοχή δινηστρίου  $0 \leq x \leq d$

$$\begin{array}{l}
 E_2 = A \sin(k_e x) e^{-j\beta z} \\
 E_x = -j\frac{\beta}{k_e} A \cos(k_e x) e^{-j\beta z} \\
 E_y = 0, H_x = 0 \\
 H_y = -j\frac{\omega \epsilon_0 \epsilon_r}{k_e} A \cos(k_e x) e^{-j\beta z} \\
 H_z = 0
 \end{array}
 \quad \left| \begin{array}{l}
 H_2 = B \cos(k_m x) e^{-j\beta z} \\
 E_x = 0 \\
 E_y = -j\frac{\omega \mu_0 \mu_r \beta}{k_m} \sin(k_m x) e^{-j\beta z} \\
 E_2 = 0, H_y = 0 \\
 H_x = j\frac{\beta}{k_m} B \sin(k_m x) e^{-j\beta z}
 \end{array} \right.$$

Χαρακτηριστικές

Ρυθμοί TM

$$k_e \tan(k_e d) = \epsilon_r h$$

$$h^2 + k_e^2 = k_0^2 (\epsilon_r \mu_r - 1)$$

Eflogies

Ρυθμοί TE

$$k_m \cot(k_m d) = -\mu_r h$$

$$h^2 + k_m^2 = k_0^2 (\epsilon_r \mu_r - 1)$$

Σταθερά της ειδότης  $\beta = 0$

$$\begin{cases} \beta^2 = h^2 + k_0^2 = 0 \\ \beta^2 = \epsilon_r \mu_r k_0^2 - k_m^2 = 0 \end{cases} \quad \left\{ \begin{array}{l} h^2 = -k_0^2 \\ k_m^2 = \epsilon_r \mu_r k_0^2 \end{array} \right.$$

$$\beta^2 = h^2 + k_0^2 = 0$$

$$\beta^2 = \epsilon_r \mu_r k_0^2 - k_m^2 = 0$$

Συχνότες Αποκοπής Επιφανειακών Ρυθμών: ( $h=0$ )

Ρυθμοί  $TM_n^2$

- Χαρακτηριστική Εφίσωση:  $\begin{cases} K_c d \cdot \tan(K_c d) = \epsilon_r h \cdot d & (1) \\ K_c^2 d^2 + h^2 d^2 = K_0^2 (\epsilon_r \mu_r - 1) d^2 & (2) \end{cases}$

- Αποκοπή Επιφανειακών Ρυθμών = Σταθερή Της Διάδοσης (Εκτετικής Επαρθένης) Γιαν αέρα:  $h=0$

- Διάγραμμα 4.19: Αποκοπή  $TM_n$ -ρυθμών:  $\leftrightarrow K_c d = n \cdot \pi = 0, \pi, 2\pi$

$$(2) \text{ για } h=0 \rightarrow K_c = K_0 \sqrt{\epsilon_r \mu_r - 1} \quad \text{Οπου } K_0 = \frac{w}{c} = \frac{2\pi f}{c}$$

$$\hookrightarrow K_c d = K_0 d \sqrt{\epsilon_r \mu_r - 1} = n \cdot \pi \quad \text{Και } n=0, 1, 2, \dots$$

$$\hookrightarrow \text{Συχνότες Αποκοπής: } \frac{2\pi f_c d \cdot \sqrt{\epsilon_r \mu_r - 1}}{c} = n \pi ; n=0, 1, 2, \dots$$

$$\left[ \begin{array}{l} P_{cn}^{TM} = \frac{n \cdot G}{2 d \sqrt{\epsilon_r \mu_r - 1}} \\ n=0 \rightarrow P_{c0}^{TM} = 0 \\ n=1 \rightarrow P_{c1}^{TM} = \frac{G}{2 d \sqrt{\epsilon_r \mu_r - 1}} \end{array} \right]$$

Ρυθμοί  $TE_n^2$

- Χαρακτηριστική Εφίσωση:  $\begin{cases} K_c d \cdot \cot(K_c d) = -\mu_r \cdot h \\ K_c^2 d + h^2 d = K_0^2 (\epsilon_r - 1) d^2 \end{cases}$

- Αποκοπή  $\leftrightarrow h=0 \rightarrow K_c^2 = K_0^2 (\epsilon_r - 1)$

$$\hookrightarrow \text{Διάγραμμα 4.20} \rightarrow K_c d = (2n-1) \frac{\pi}{2} \quad \text{για } n=1, 2, 3, \dots$$

$$\hookrightarrow \text{Συχνότης αποκοπής: } P_{cn}^{TE} = \frac{(2n-1) G}{4d \sqrt{\epsilon_r - 1}} \quad \text{για } n=1, 2, 3, \dots$$

Αποκύψη Της Διέρευνης στην ΤΕ ρυθμού:

$$P < P_{c1}^{TE} = \frac{G}{4d \sqrt{\epsilon_r - 1}} \quad \text{d} \leq \frac{C}{4f \sqrt{\epsilon_r - 1}} = \frac{20}{4f \sqrt{\epsilon_r - 1}}$$

Επιλογή Πλάκας  $20 \times 30$  mm:  $d < \frac{20}{4 \sqrt{\epsilon_r - 1}} = \frac{C}{4f \sqrt{\epsilon_r - 1}}$

Παράδειγμα:  $\epsilon_r = 3.38$   $\left\{ \begin{array}{l} d \leq 4.86 \text{ mm} \\ f = 10 \text{ GHz} \end{array} \right.$

$$\Rightarrow \epsilon_r = 9.6 \text{ (Αναλύτικη)} \rightarrow d \leq 2.56 \text{ mm}$$

TM

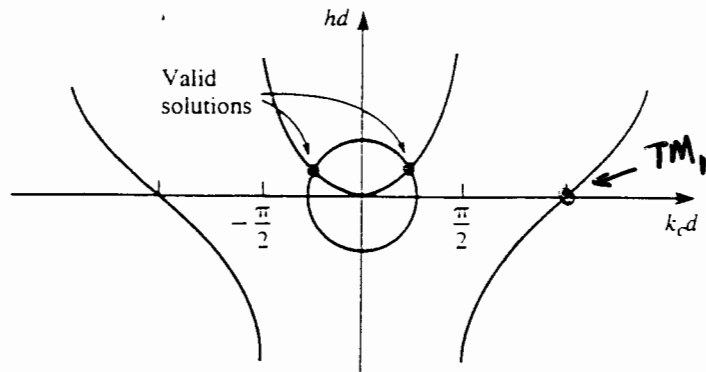


**FIGURE 4.19** Graphical solution of the transcendental equation for the cutoff frequency of a TM surface wave mode of the grounded dielectric slab.

TE

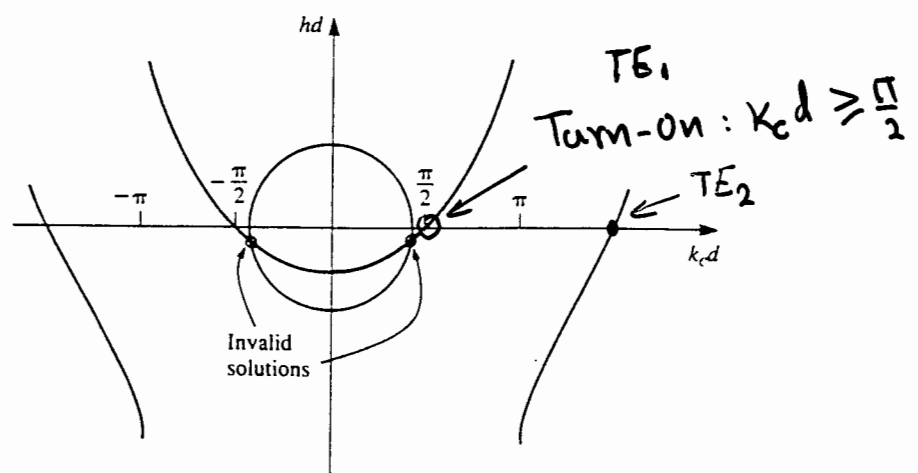


**FIGURE 4.20** Graphical solution of the transcendental equation for the cutoff frequency of a TE surface wave mode. Figure depicts a mode below cutoff.

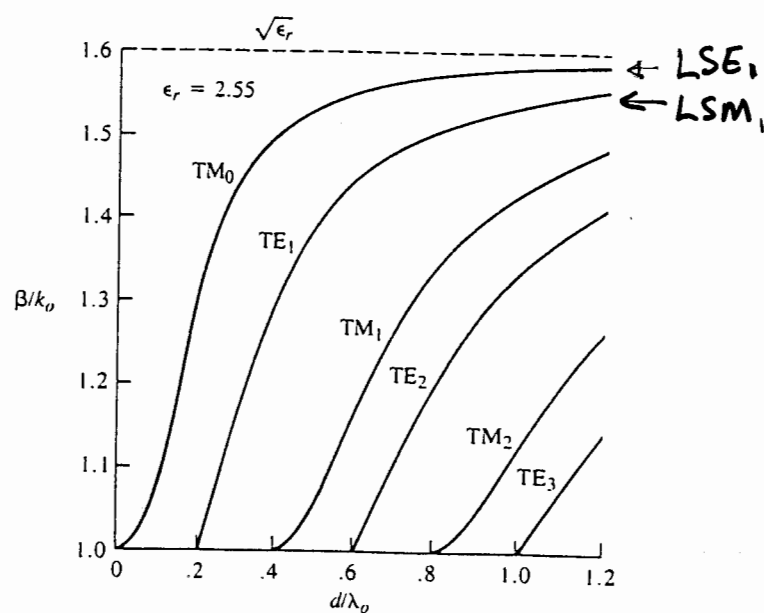
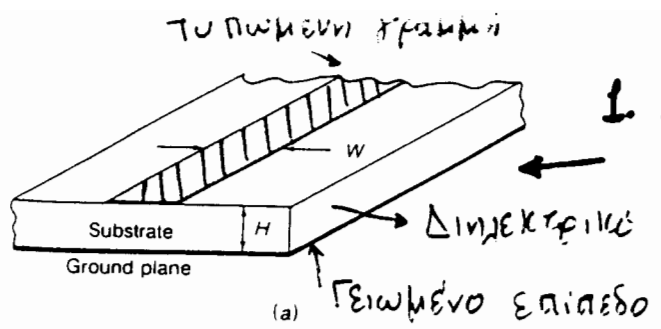


**FIGURE 4.21** Surface wave propagation constants for a grounded dielectric slab with  $\epsilon_r = 2.55$ .



1. Μικροστριπ γραφική  
(Microstrip Line)

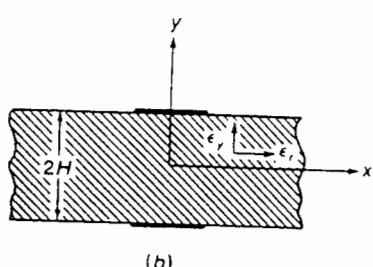


FIGURE 3.17

(a) The microstrip transmission line  
(b) equivalent parallel strip line obtained by using image theory.

ΟΠΟΚΛΗΡΩΜΕΝΕΣ -  
- ΤΥΠΩΜΕΝΕΣ ΜΙΚΡΟΚΥΜΗΣ ΓΡΑΜΜΕΣ ΜΕΤΑΦΟΡΑΣ

Συζευγμένες μικροστριπές γραφικές

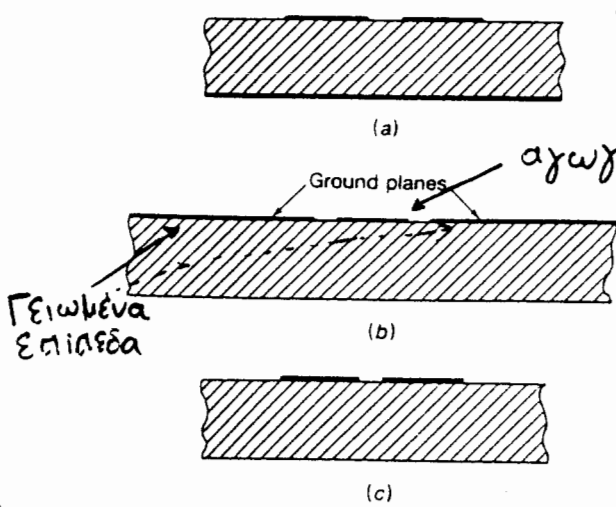
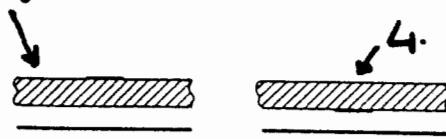


FIGURE 3.18

(a) Coupled microstrip lines; (b) coplanar transmission line; (c) coplanar strip transmission line.

3. ΥΠΕΡΥΨΗΜΕΝΗ ΜΙΚΡΟΣΤΡΙΠ ΓΡΑΦΙΚΗ (Suspended microstrip)

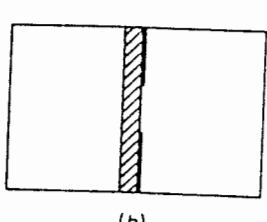


4. ΑΝΕΞΤΡΑΠΗΜΕΝΗ ΜΙΚΡΟΤ. ΓΡΑΦΙΚΗ (Inverted microstrip)

FIGURE 3.19  
Suspended and inverted suspended microstrip line.



5. ΣΧΙΣΜΟΣΙΔΟΣ ΓΡΑΦΙΚΗ (Slot line)



6. Θωρακισμένη σχισμοσίδος γραφική  
(Shielded slot line or Fin line)

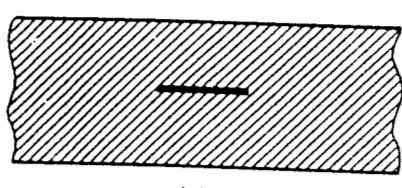


FIGURE 3.20  
(a) Slot line; (b) shielded slot line or fin line; (c) stripline.

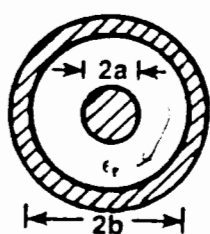
7. Ταινιογραφική (Stripline)

# RF - MICROWAVE TRANSMISSION LINES

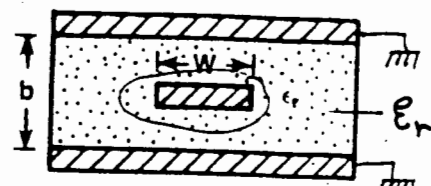
## Conventional

$$\beta = w\sqrt{\mu\epsilon}$$

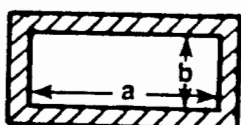
Coaxial Line



Strip Line

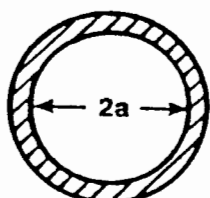


Rectangular Waveguide



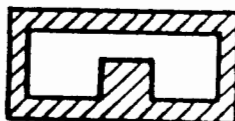
MICs  
MMICs

Cylindrical Waveguide

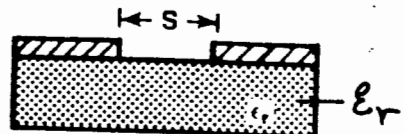


MICs → Slot Line  
{ high Imp. Lines,  
Series Stubs, ... }

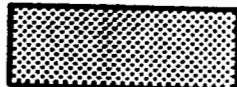
Ridged Waveguide



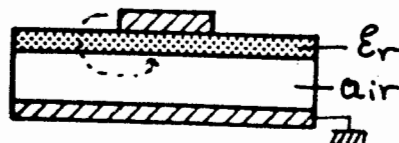
MICs  
CPW  
? MMICs ?



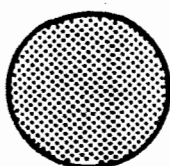
Rectangular Dielectric Waveguide



Suspended Microstrip  
Or inverted



Cylindrical Dielectric Waveguide



Fin Line

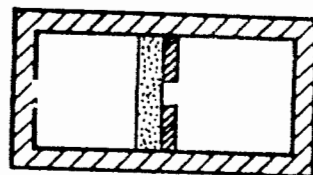


Figure 2.2 Transmission structures for microwave circuits.

⇒ Half Wavelength  $\lambda_g/2$ , Quarter Wavelength  $\lambda_g/4$  or smaller Sections of these lines form the basic building blocks in Most Microwave Circuits.

$$\lambda_g = \frac{2\pi}{\beta} = \frac{2\pi}{K_0 \sqrt{\epsilon_{eff}}} = \frac{2\pi}{2\pi/20 \cdot \sqrt{\epsilon_{eff}}} = \frac{20}{\sqrt{\epsilon_{eff}}} \Rightarrow \lambda_g = \frac{20}{\sqrt{\epsilon_{eff}}} = \frac{C}{f \sqrt{\epsilon_{eff}}}$$

Size Reduction using High Dielectric Const.  $\epsilon_r$

Alumina  $\text{Al}_2\text{O}_3$  | GaAs → MMICs | Si  
 $\epsilon_r = 9.9, \tan\delta = 10^4$  |  $\epsilon_r = 12.9, \tan\delta = 6 \cdot 10^4$  |  $\epsilon_r = 12, \tan\delta = 10^3 \rightarrow 10^{-2}$  |  $\epsilon_{eff} < \epsilon_r$

# INTEGRATED MICROWAVE TRANSMISSION LINES

**Strip Line**: TEM dominant mode.

- Simple analytical expressions  $\leftrightarrow$  Electrostatic analysis
- difficult fabrication

**Microstrip** quasi-TEM dom. mode MICs and MMICs

- Approximate Quasi-Static models  $\rightarrow$  Closed form expr.
- $\Rightarrow$  → Almost exclusively used in MMICs { $Z_0, \epsilon_{eff}$ }
- $\Rightarrow$  → Convenient only in series mounting

**Suspended and Inverted Microstrip Lines**

- Higher Q than Microstrips
- Wide range of Impedance values  $\Rightarrow$  Particularly Suitable for filters

**Slot Line** dominant mode  $\rightarrow$  Almost TE  $\Rightarrow$  MIC

- Useful in circuits requiring high Impedance lines, Series Stubs, Short Circuits

$Z_0, \lg$  approximate expressions by curve fitting the numerical results

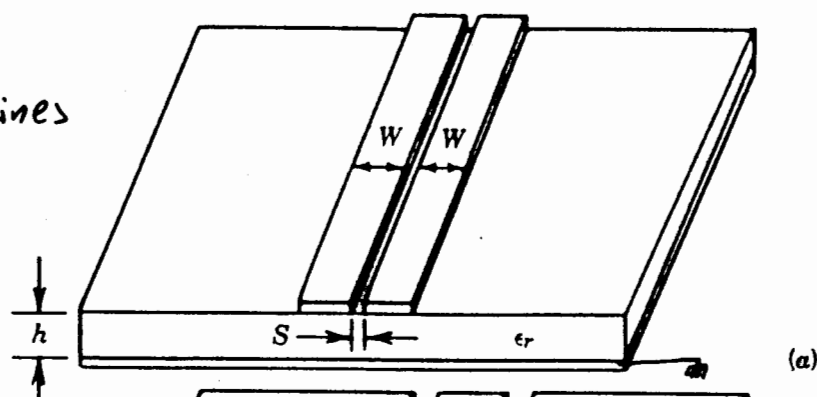
- $\Rightarrow$  • Convenient only in Shunt mounting

**Coplanar Lines** C.P.W., dominant mode is Quasi TEM

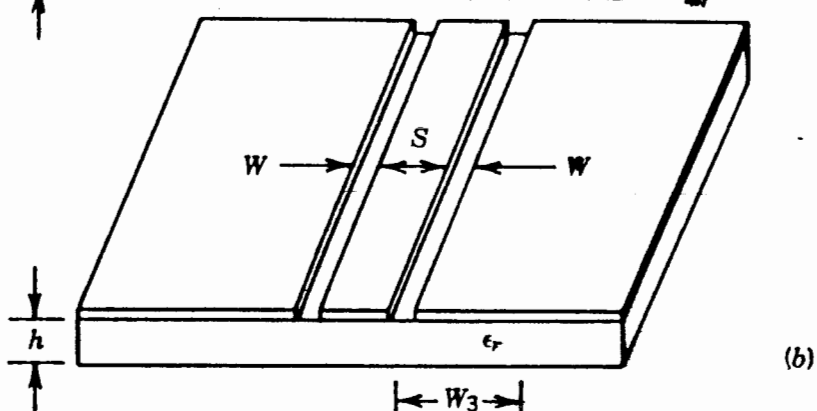
- + • Extensive applications in MICs
- + • Flexibility in Circuit design
- + • Avoiding vias for grounding (drilling holes)
- (-) • Difficulties in the analysis  $\rightarrow$  Available Approx. expr. for  $Z_0, \epsilon_{eff}$
- Combine Microstrip and Slot line advantages
  - only series mounted comp.  $\rightarrow$  Only shunt mounted components
- Interest for use in MMICs

## Coupled Lines

Coupled  
Microstrip Lines



Coupled  
Slotlines



Coupled Coplanar  
Waveguides

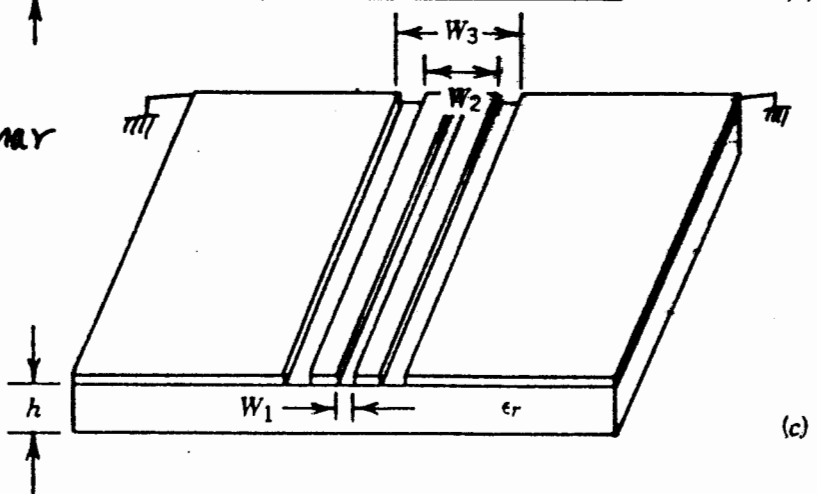


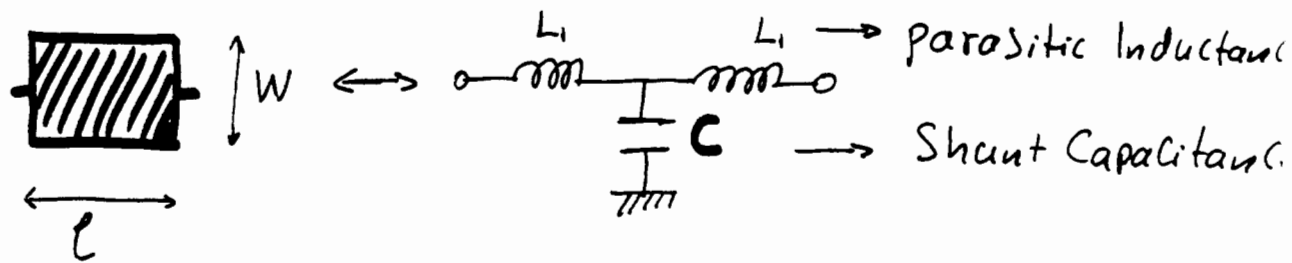
Figure D.9 Configurations of (a) coupled microstrip lines; (b) coupled slotlines; and (c) coupled coplanar waveguides.

**Coupled Lines → Basic Elements for :**

- directional Couplers      • Filters
- Phase Shifters            • Baluns
- Due to Coupling they Support two different Modes of propagation
- Even Modes  $Z_{oe}, V_{pe}, E_{eff,e} \}$   $\Rightarrow$  Desirable property
- Odd Modes  $Z_{oo}, V_{po}, E_{eff,o} \}$   $\Rightarrow$  for the design of Directional Couplers

# Microstrip Capacitors MICs and MMICs

Wide Microstrip Lines (or Stubs) = Shunt Capacitor.

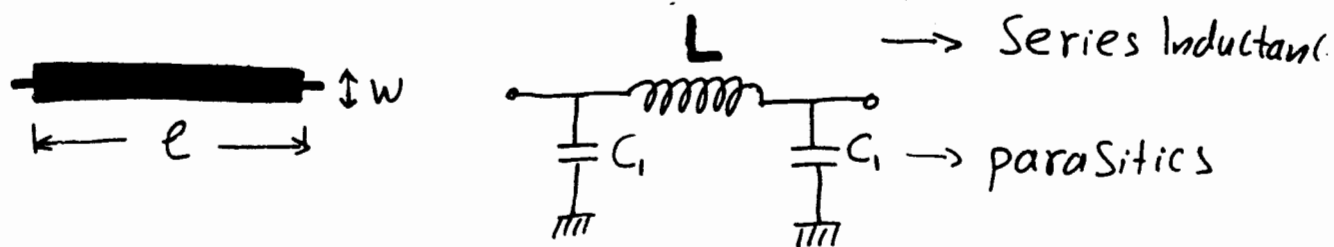


$$0 \leq C \leq 0.1 \text{ pF} \quad \text{design: } l \approx \frac{\lambda g}{2\pi} \cdot \sin^{-1}(w.c. Z_0)$$

$$\frac{L}{2} = L_1 = \frac{Z_0}{2w} \sin\left(\frac{2\pi l}{\lambda g}\right)$$

# Microstrip Inductors MICs and MMICs

Narrow Microstrip Lines

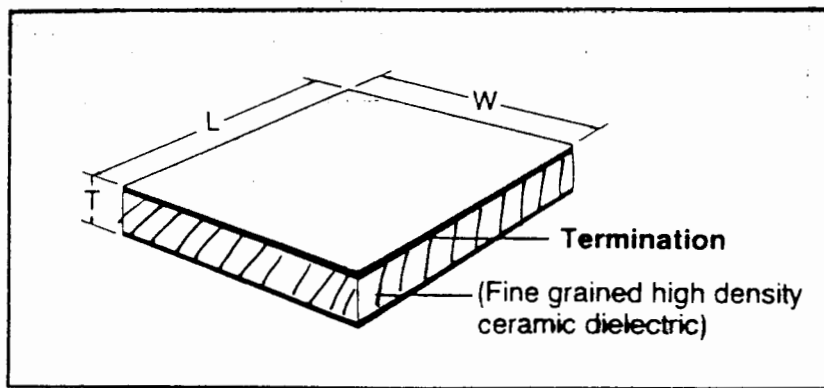


$$L \leq 2 \text{ to } 3 \text{ nH} \quad \text{design: } l \approx \frac{\lambda g}{2\pi} \sin^{-1}\left(\frac{\omega L}{2\pi}\right) \leftarrow Z_0$$

$$C_1 = \frac{C}{2} = \frac{1}{2\omega Z_0} \tan\left(\frac{\pi l}{\lambda g}\right)$$

# CHIP CAPACITORS → USED in Hybrid MICs

Single-layer



Metal - Insulator - Metal



MIM

$$0.1\text{pF} \leq C \leq 25\text{pF}$$

Multi-layer

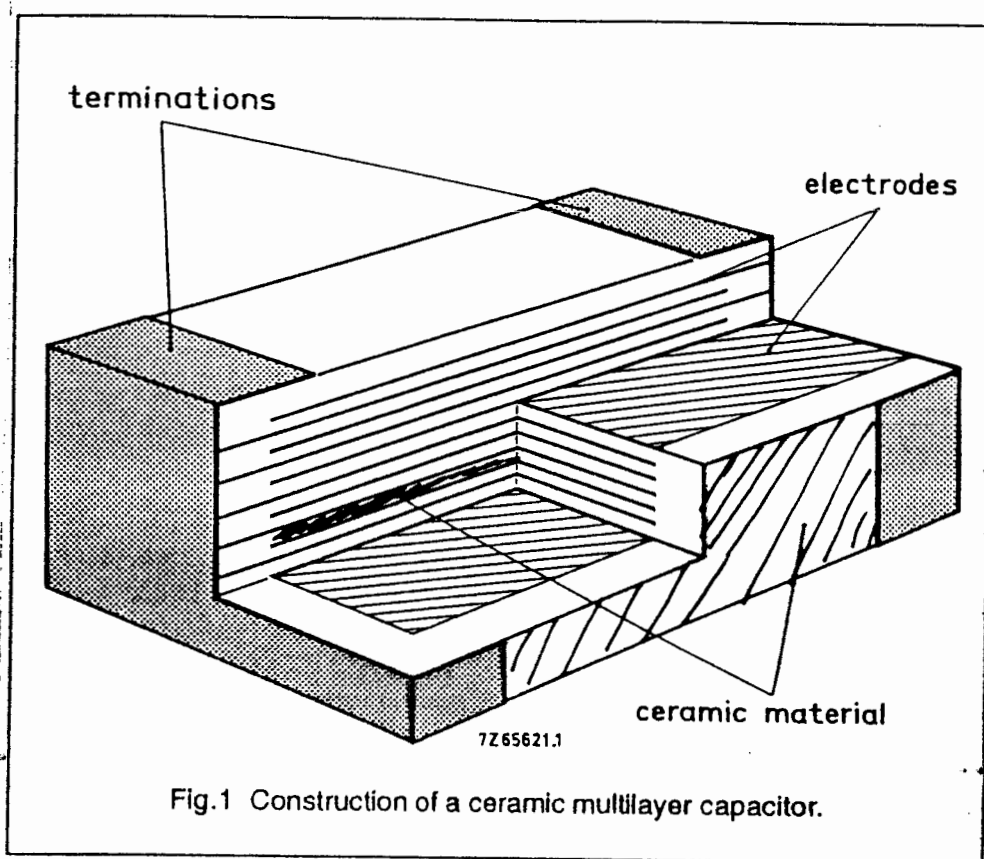
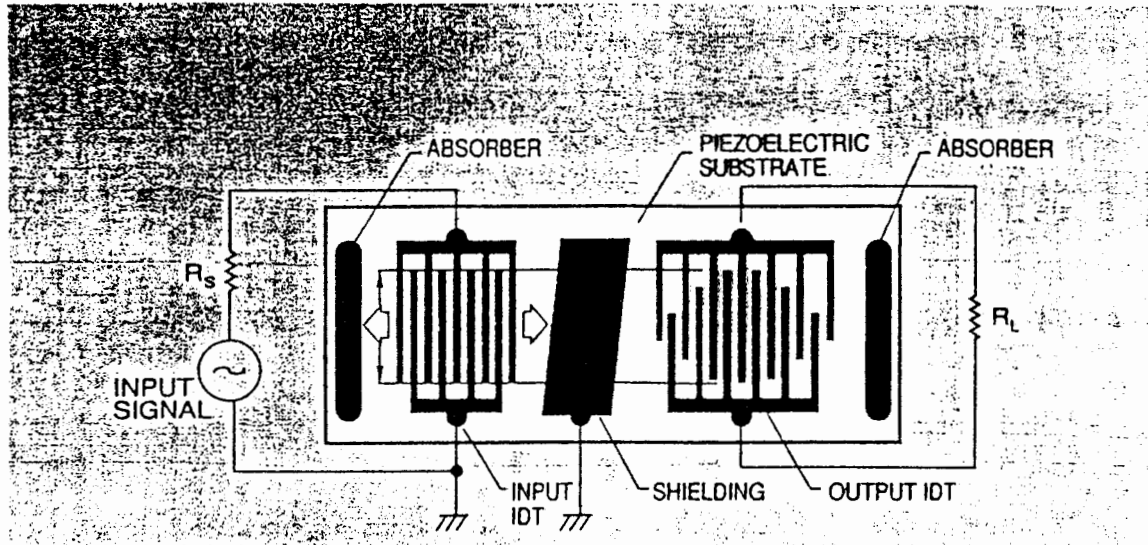


Fig.1 Construction of a ceramic multilayer capacitor.

## SAW FILTERS (Band-Pass)



#### D.4 MONOLITHIC ELEMENTS for MMICs

## Interdigital Capacitor

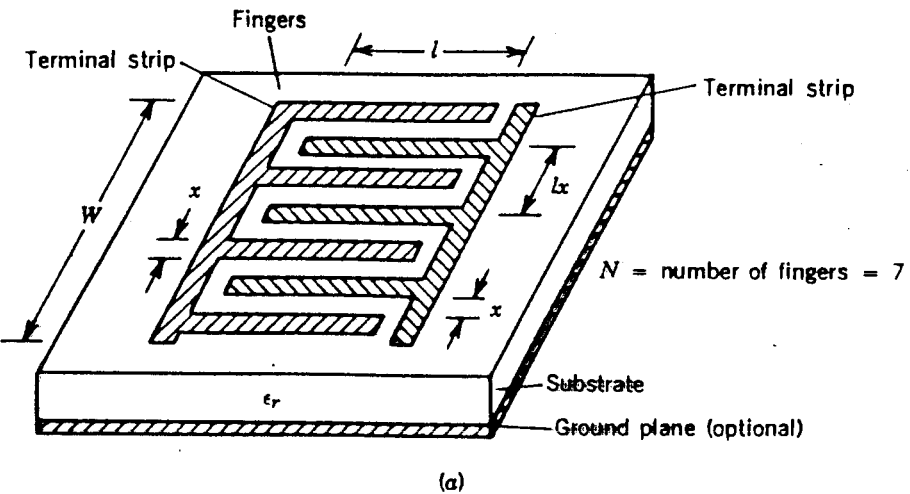


**Figure D.22** (a) Configuration of an interdigital capacitor.

$$0.05 \text{ pF} \leq C \leq 0.5 \text{ pF}$$

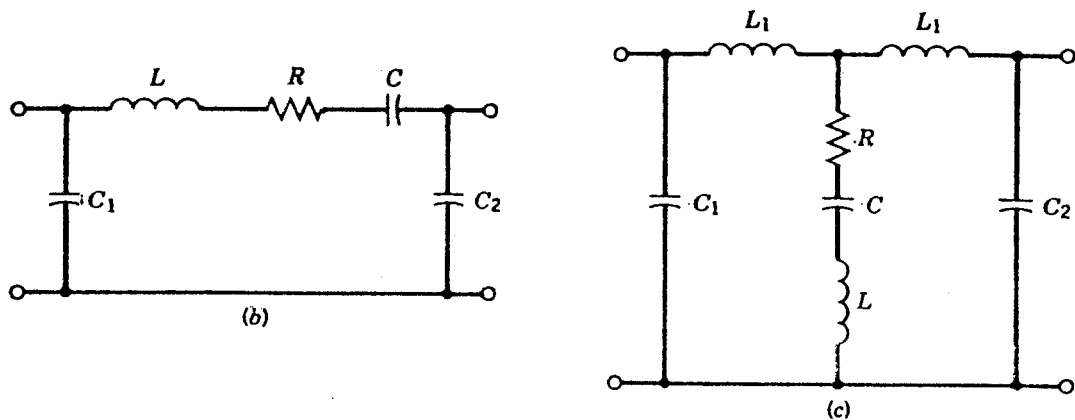


**Figure D.22** (b) Equivalent circuit for series mounting; (c) Equivalent circuit for shunt mounting.

**Methods:** The capacitance between two sets of digits in interdigital structure is found by using the capacitance formula for the odd mode in coupled microstrip lines, with the ground plane spacing tending to an infinitely large value.

### - Schottky Junction Capacitors

$0.5\text{ pF} \leq C \leq 100\text{ pF}$       Voltage dependent

## -Metal - Insulator - Metal M.I.M capacitors

$$0.1 \text{ pF} \leq C \leq 25 \text{ pF}$$

## Interdigital Rectangular and Spiral Inductor

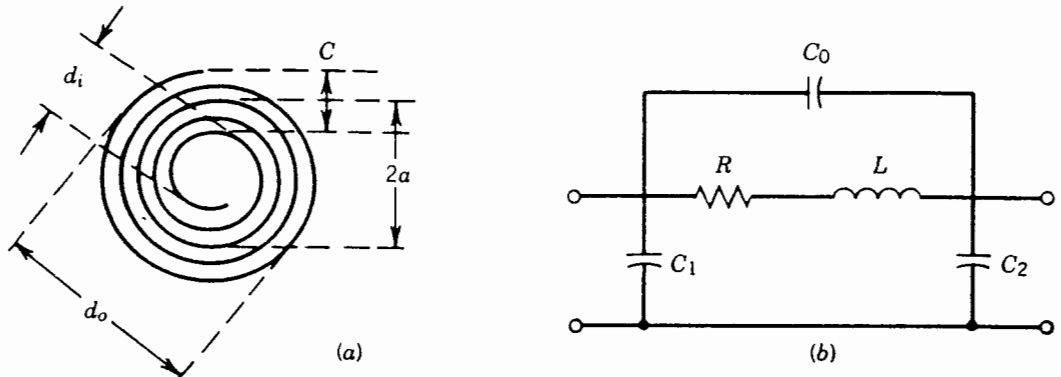


**Figure D.23** (a) Configuration of a spiral inductor; (b) Equivalent circuit for a spiral inductor.

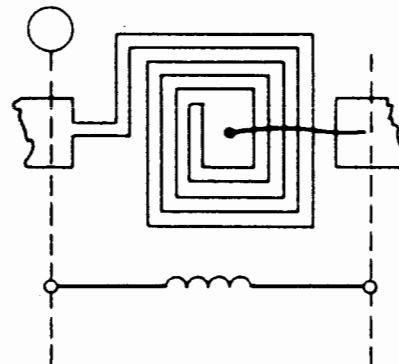


**Figure D.24** Interdigital rectangular inductor layout and the equivalent circuit.

## Interdigital transformer

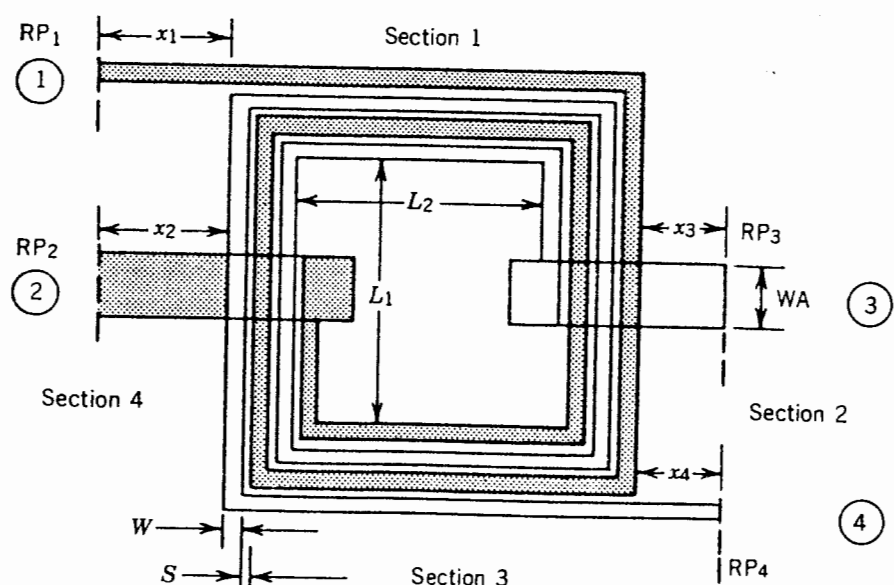
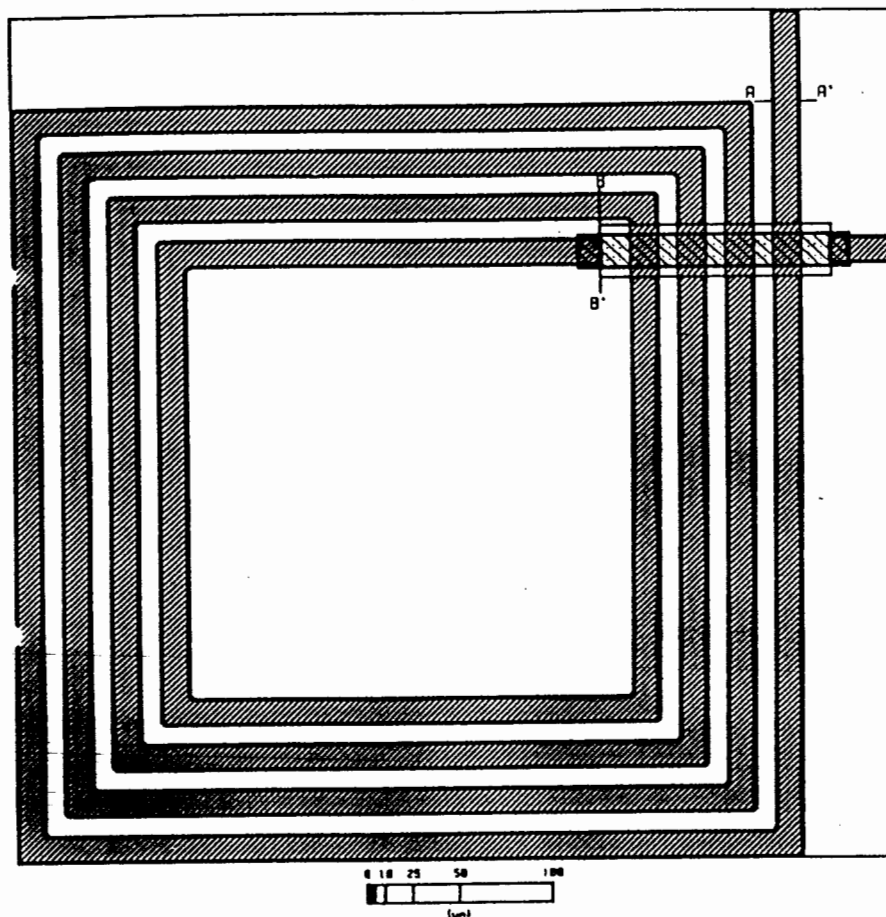


**Figure D.25** Geometry parameters for the module PLTRAN describing the general transformer geometry.

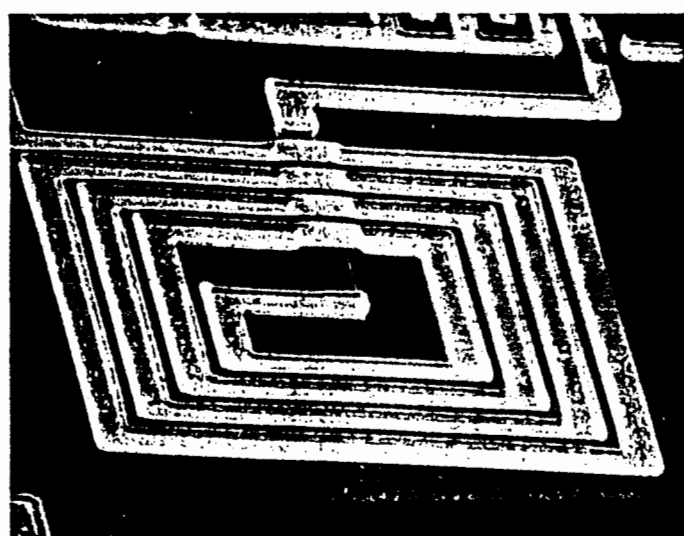
# GaAs MMIC Spiral Inductor

GALLIUM ARSENIDE MONOLITHIC I



Layout

Figure 8.5 Standard four-turn spiral inductor layout.



photograph

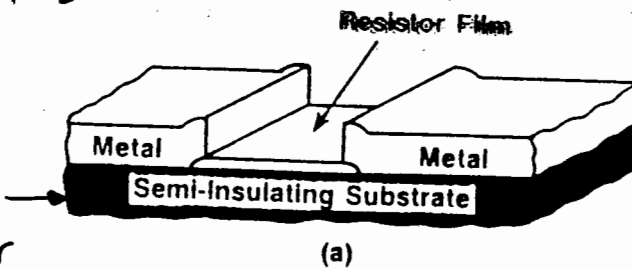
Figure 8.6 Scanning electron micrograph of a four-turn inductor.

# MICs or MMICs Resistors

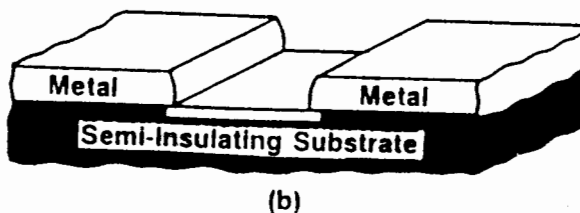
**Thin Film**

Dielectric

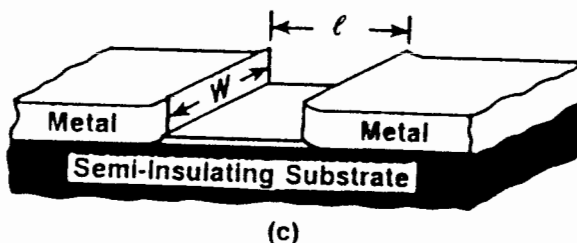
or Semiconductor



**mesa-type**



**Implanted**



Chip Resistors  
are usually used  
in MICs  
(Hybrid MICs).

MICs  $\rightarrow$  dielectri

- Nichrome
- Tantalum Nitrid

MMICs

GaAs, Si

Figure 2.23 Planar resistors. (a) Thin-film. (b) Mesa. (c) Implanted.

$$R \approx R_s \frac{l}{w}$$

$$\text{OR} \quad R = \rho_s \frac{l}{dW} \quad (2.37b)$$

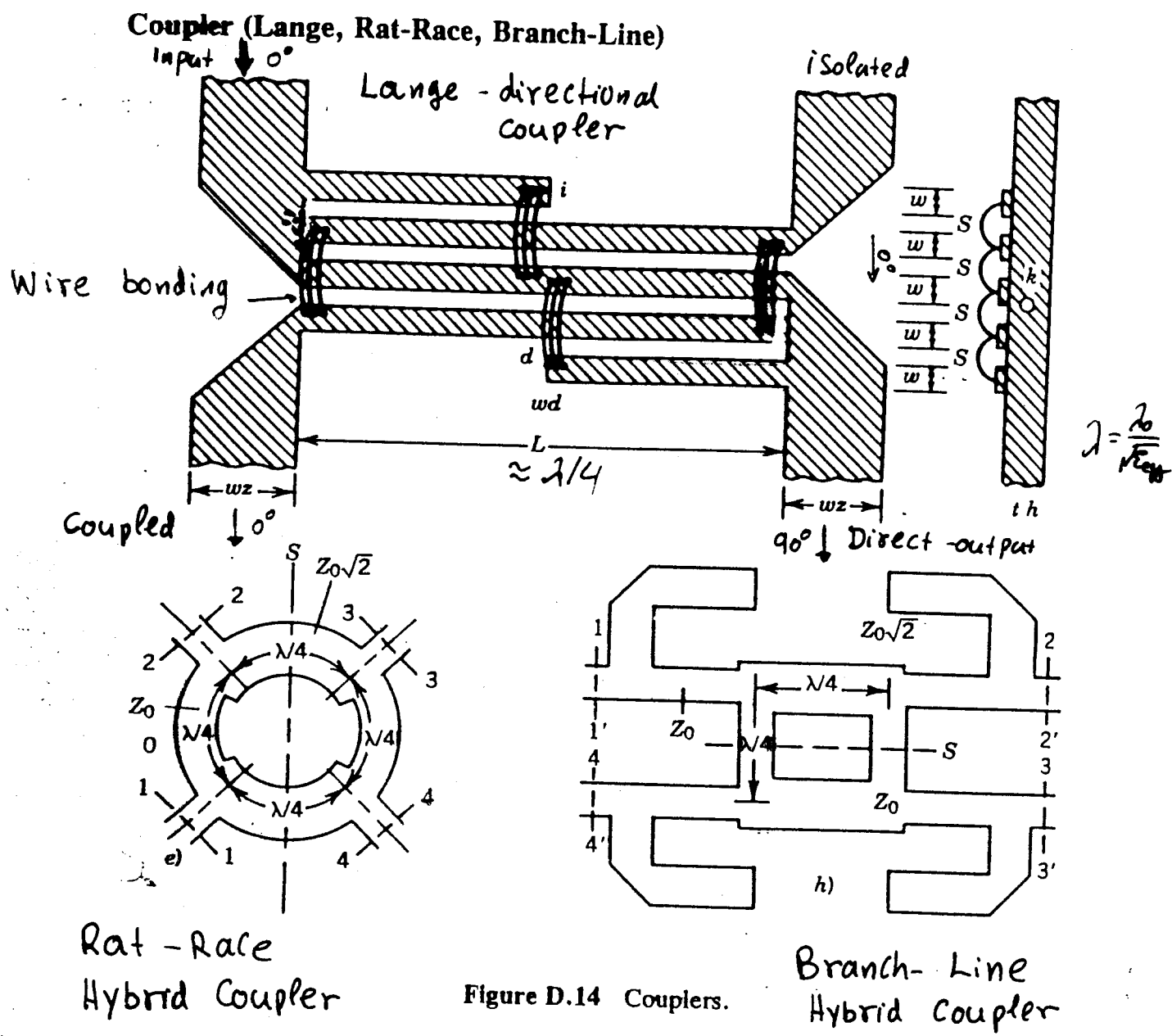
Here  $R_s$  is the surface resistance ( $\Omega/\text{square}$ ) and  $\rho_s$  is the specific resistivity ( $\Omega\cdot\text{m}$ ) of the resistor film. The thickness  $d$ , width  $W$ , and length  $l$  of the film are measured in meters. The capacitance can be determined from the microstrip-line considerations. When film thickness  $d \geq 1 \mu\text{m}$ , the formula containing  $R_s$  should be used. However, for very thin films,  $d \leq 1 \mu\text{m}$ , the formula with  $\rho_s$  should be used. Desirable characteristics of film resistors are

- good stable-resistance value, which should not change with time,
- low temperature coefficient of resistance (TCR),
- adequate dissipation capability,
- sheet resistivities in the range of 10 to 1000  $\Omega/\text{square}$ , so that parasitics can be minimized,
- maximum resistor length less than  $0.1\lambda$  if transmission line effects are to be ignored.

$\rho_s$

$l$

# MICs and MMICs Couplers



**Description:** There are two kinds of couplers. Directional couplers and hybrid couplers (such as rat-race and branch-line)

# ACTIVE DEVICES → MICs

**3.2.3 MODFET/HEMT Modulation Doped FET / High Electron Mobility Transistor**

By using heterojunction semiconductor material, AlGaAs interfacing with GaAs, a new field-effect microwave semiconductor device can be manufactured with

## HEMT

Operation  
frequently  
up to  
60 GHz

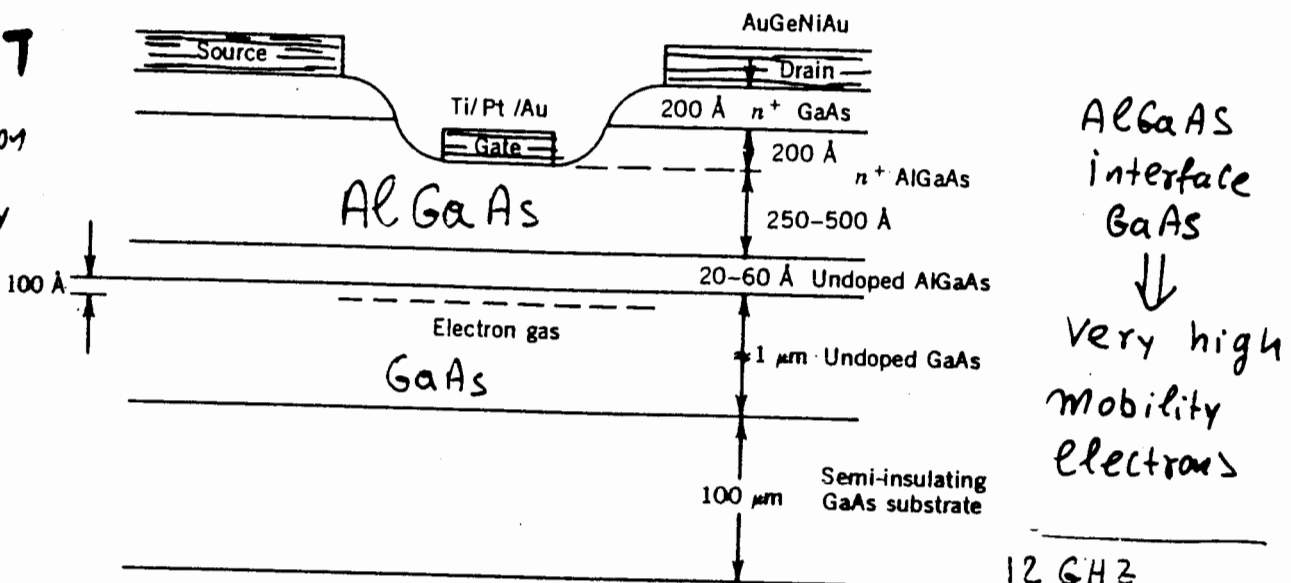


Figure 3.23 MODFET/HEMT structure. (From Refs. 3.1 and 3.58.)

superior microwave performance. This device is the MODFET (modulation-doped field-effect transistor), which is also called a HEMT (high electron mobility transistor), a SDHT (selectively doped heterostructure transistor), or a TEGFET (two-dimensional electron gas FET); the cross section of this transistor is given in Fig. 3.23 [3.58, 3.1].

## MESFET → Metal - Semiconductor Field Effect Transistor

Operating  
up to  
~ 186 Hz

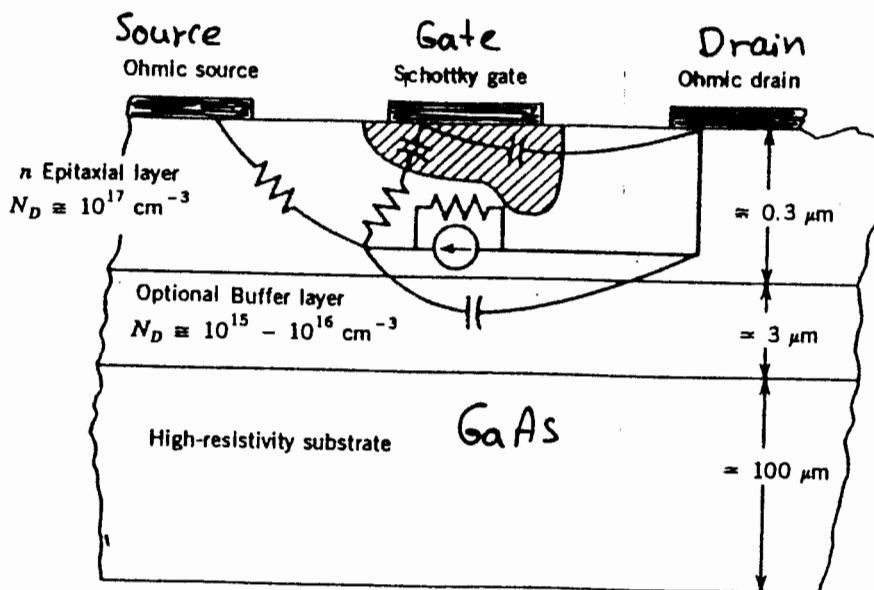


Figure 3.11 GaAs MESFET cross section.

- + Very low noise figure  $F_{min} = 0.5 \text{ dB}$  at  $4 \text{ GHz} \leftrightarrow P_{out} = 15 \text{ W}$   
(Silicon Bipolar  $F_{min} = 2.5 \text{ dB}$  at  $4 \text{ GHz}$ )  $\leftrightarrow P_{out} = 6 \text{ W}$
- (-) 1/f Corner frequency  $30 \text{ MHz}$ ; ( $\text{Si-HBT} \rightarrow 10 \text{ kHz}$ )

### 3.1.4 Heterojunction Bipolar Transistor

HBT

Because of the superior material properties of group III-V compounds such as GaAs, a bipolar transistor using this material has been a goal since 1957 [3.22]. The use of the heterojunction emitter-base has made the heterojunction bipolar transistor (HBT) a reality. Three primary advantages result from this structure (Fig. 3.8) [3.23]:

1. The forward-bias emitter injection efficiency is very high since the wider-bandgap AlGaAs emitter injects electrons into the GaAs base at a lower operating up to 60 GHz

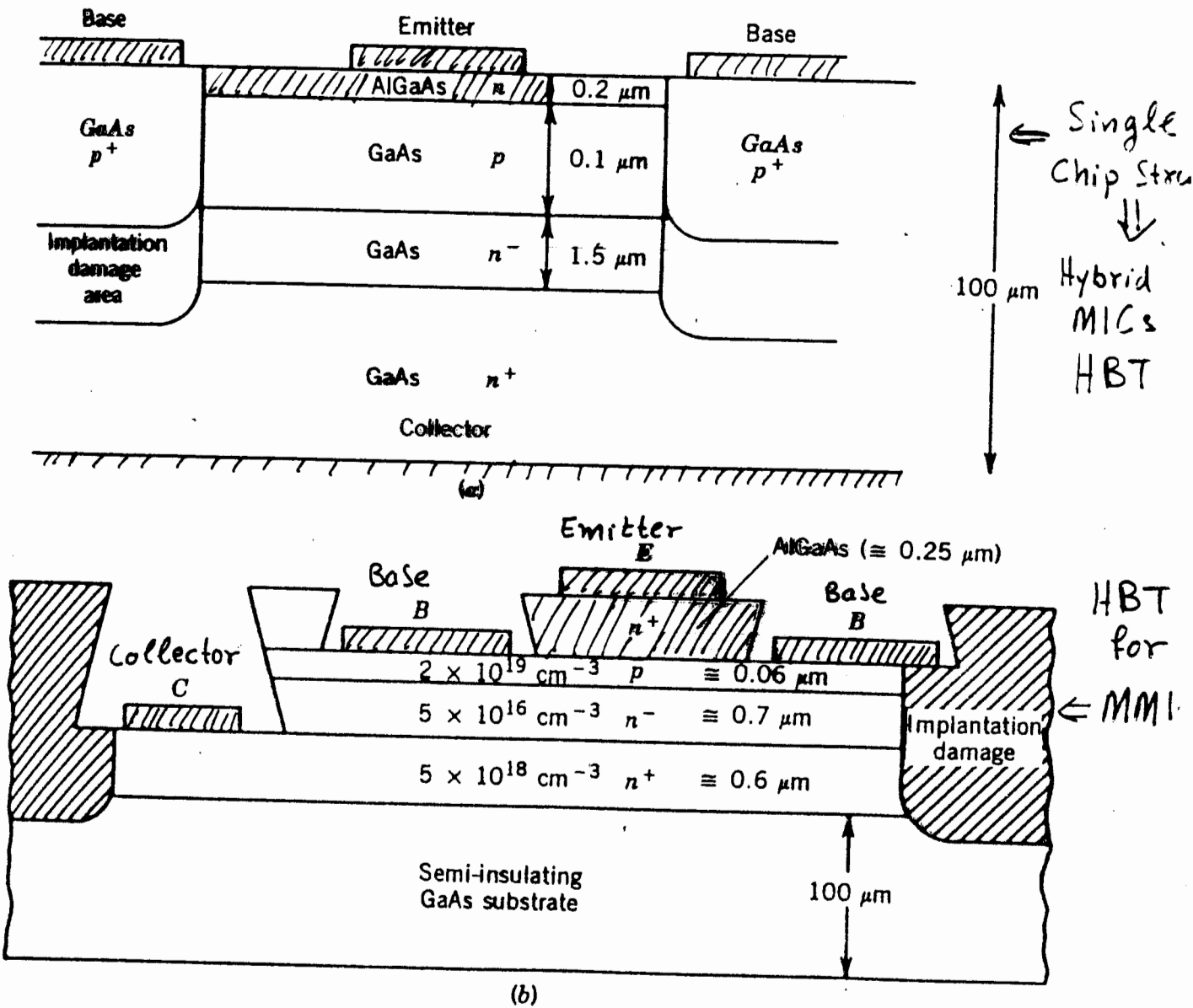


Figure 3.8 Heterojunction bipolar transistor structure (HBT): (a) single-chip structure; (b) HBT structure for GaAs monolithic circuits. [(b) from Ref. 3.23.] © 1987 IEEE.

+ 1/f Corner Frequency 1 MHz !! (very low)

- + Power density 1.5 mW/mm at 36 GHz
- High Noise Figure  $F_{min} = 4 \text{ dB}$  at 20 GHz
- A very promising microwave transistor.

# MESFET versus Si-BJT NOISE PERFORMANCE

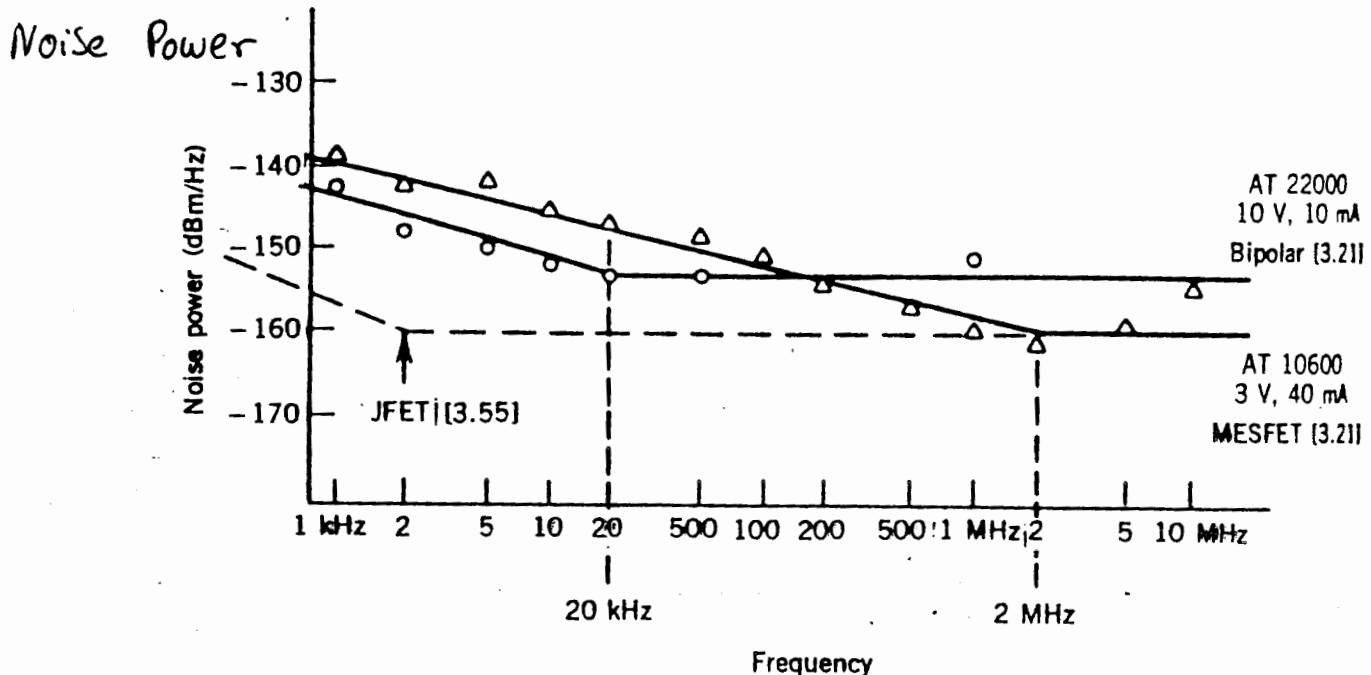


Figure 3.21  $1/f$  noise for microwave transistors. (From Refs. 3.21 and 3.55.)

transistors has been plotted in Fig. 3.22 for room temperature. The GaAs MESFETs will dominate the microwave region, but silicon bipolars will continue to find applications, especially for low-noise oscillators.

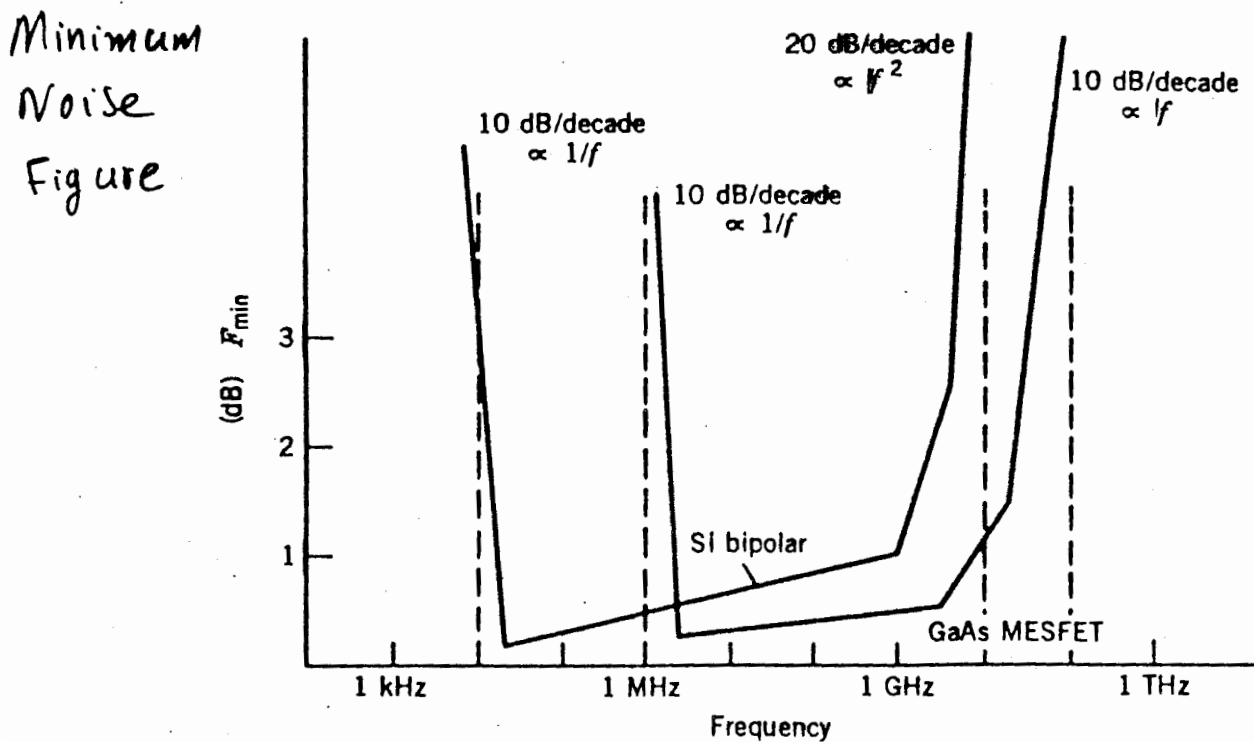


Figure 3.22  $F_{\min}$  versus frequency for low-noise silicon bipolar transistor and for noise gallium arsenide FET.

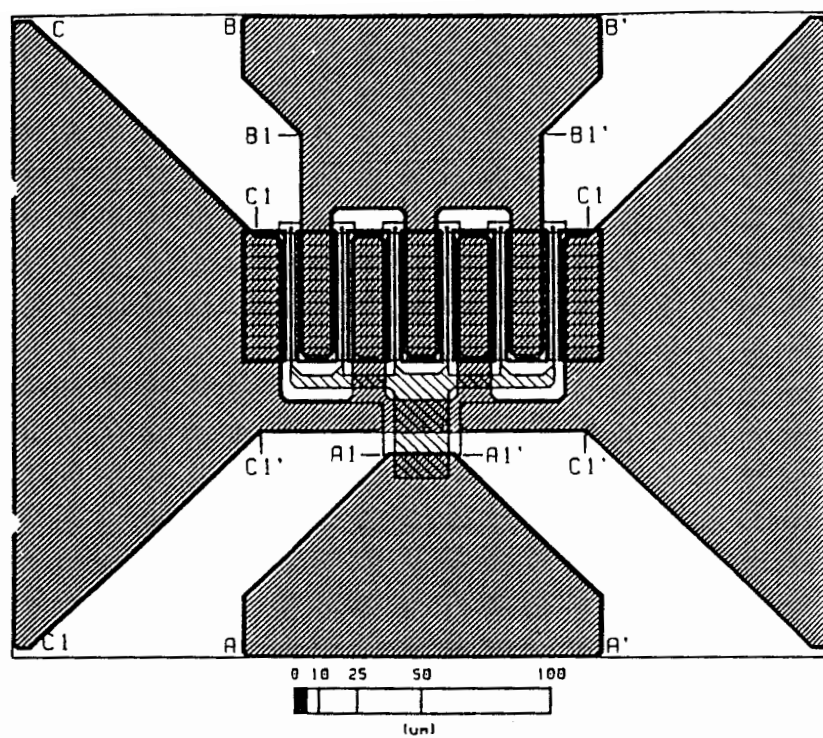
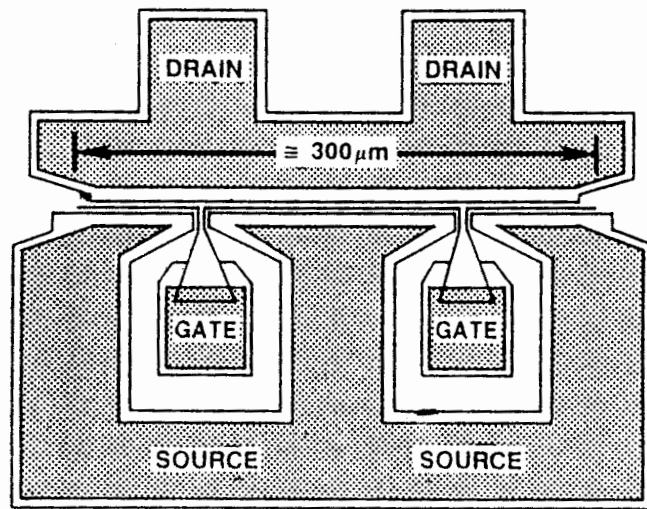


Figure 8.4 Standard  $0.5\text{-}\mu\text{m}$  gate length FET layout.



(a)

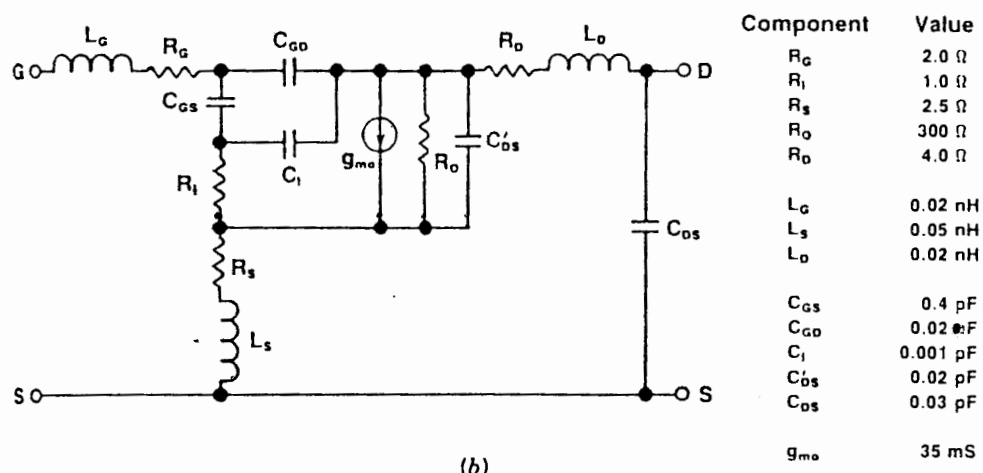
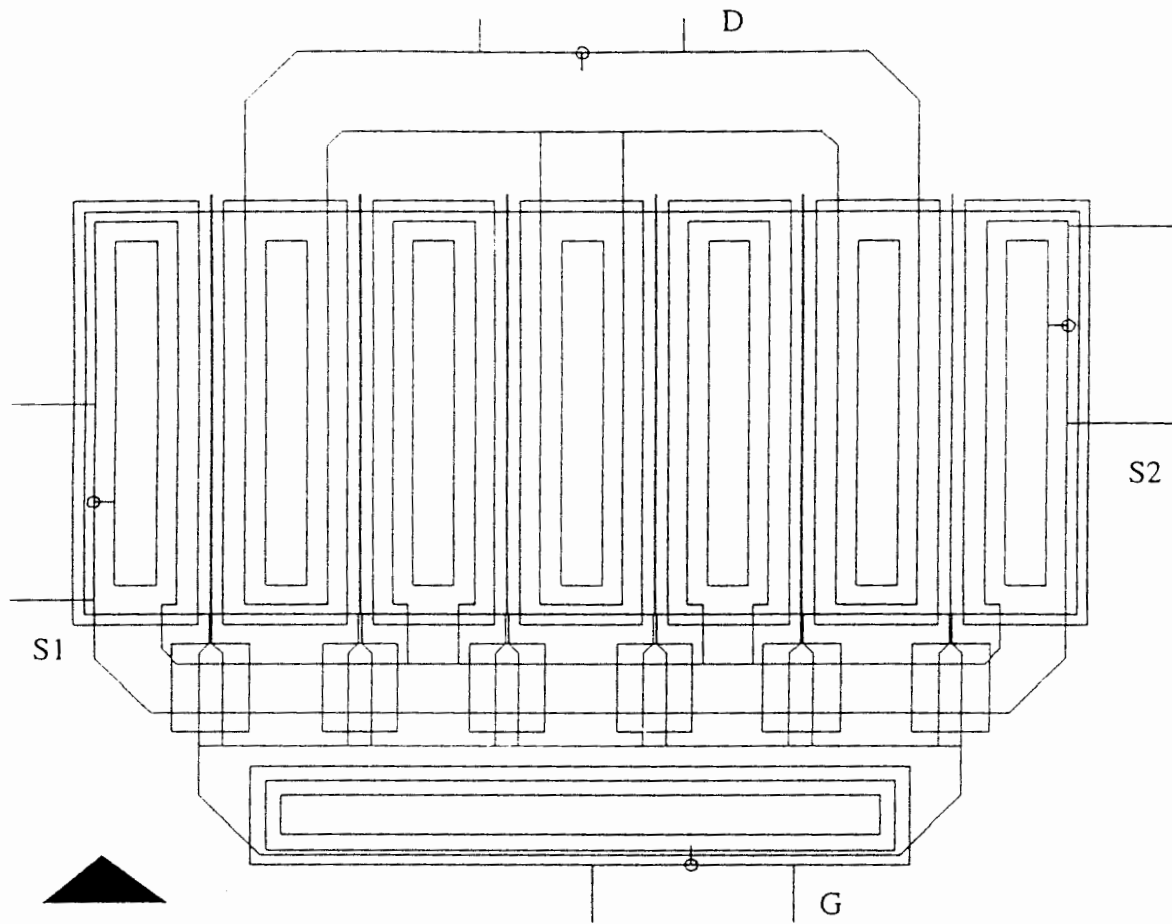
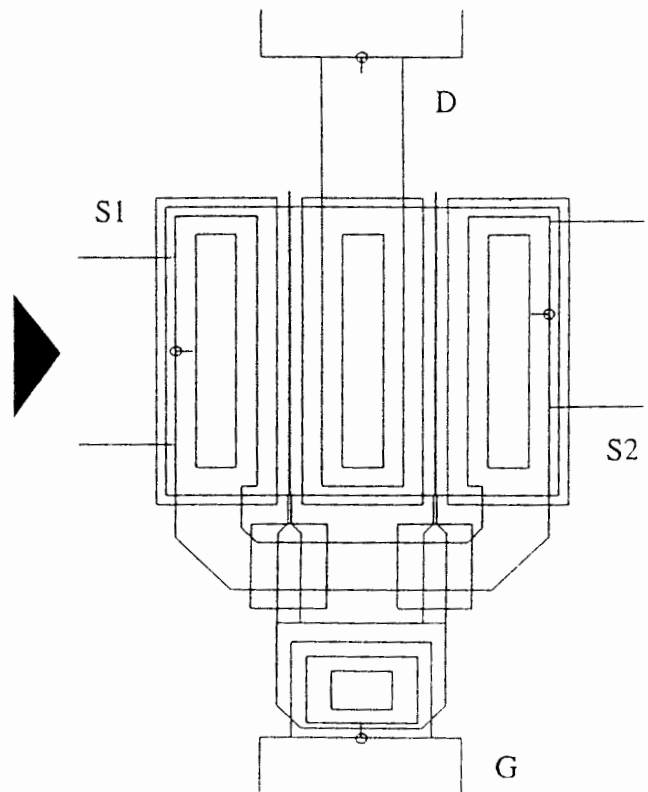


Figure 10.11 (a) Four-finger MESFET configuration. (b) Equivalent circuit.

**Layout Examples :**

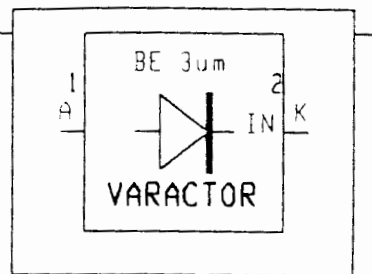
$N_{bd} = 6$   
 $W_u = 40 \mu m$   
 $W_g = 20 \mu m$   
 $P_g = 0.5$   
 $W_d = 20 \mu m$   
 $P_d = 0$   
 $W_{s1} = 20 \mu m$   
 $P_{s1} = -1$   
 $W_{s2} = 20 \mu m$   
 $P_{s2} = 1$

$N_{bd} = 2$   
 $W_u = 30 \mu m$   
 $W_g = 20 \mu m$   
 $P_g = 1$   
 $W_d = 20 \mu m$   
 $P_d = 0$   
 $W_{s1} = 20 \mu m$   
 $P_{s1} = 0$   
 $W_{s2} = 20 \mu m$   
 $P_{s2} = 1$



## EDDIBE

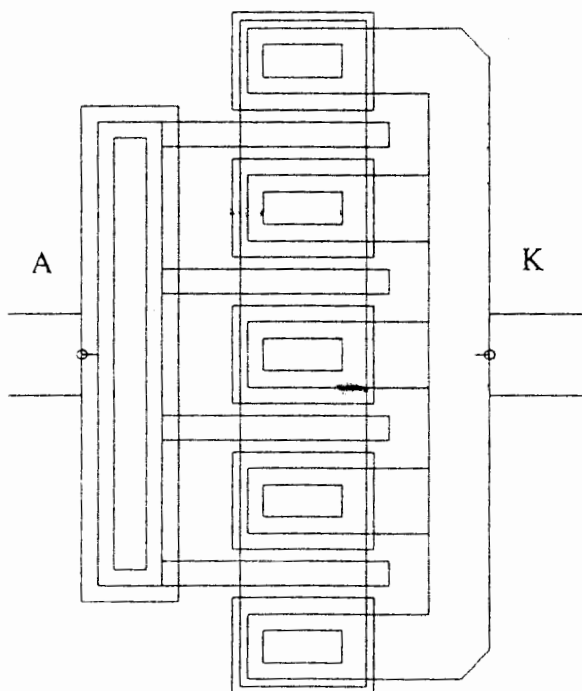
**Description :** Large signal model of BE diode.

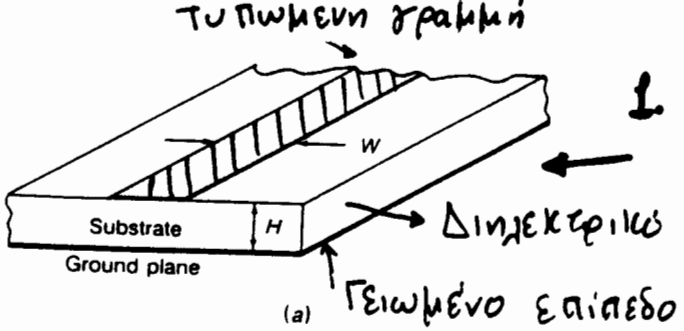


**Arguments :**

Name	Default	Description
Nbd	4	Number of gate fingers.
Wu	15 $\mu\text{m}$	Width of an individual gate finger.
Wa	10 $\mu\text{m}$	Anode access line width.
Pa	0	Lateral position of the anode access line (-1 < Pa < 1).
Wk	10 $\mu\text{m}$	Cathode access line width.
Pk	0	Lateral position of the cathode access line (-1 < Pk < 1).

**Layout Example :** Nbd = 4, Wu = 15  $\mu\text{m}$  :





1. Μικροστριπ γραμμή<sup>1</sup>  
(microstrip line)

Γειωμένο επίπεδο

## ΟΠΟΚΛΗΡΩΜΕΝΕΣ - ΤΥΠΩΜΕΝΕΣ ΜΙΚΡΟΚΥΜ ΓΡΑΜΜΕΣ ΜΕΤΑΦΟΡΑΣ

FIGURE 3.17

(a) The microstrip transmission line  
(b) equivalent parallel strip line obtained by using image theory.

## Συγεγριθέντες μικροστριπές γραμμές



(a)

αγωγός σημάτος



(b)



(c)

## 2. Ομοεπιπέδες Γραμμές (η κυριότερη) (Coplanar waveguides)

FIGURE 3.18

(a) Coupled microstrip lines; (b) coplanar transmission line; (c) coplanar strip transmission line.

## 3. Υπερυγωμένη μικροστριπές γραμμή (Suspended microstrip)

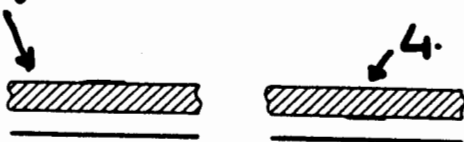
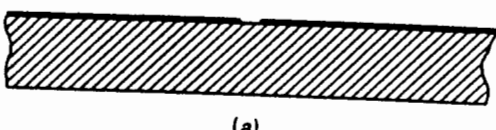
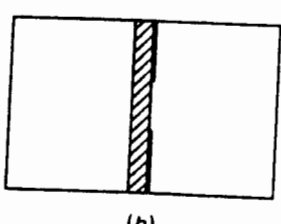


FIGURE 3.19  
Suspended and inverted suspended microstrip line.

## 5. Σχιζμοειδής Γραμμή (Slot line)



(a)



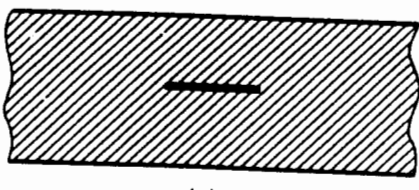
(b)

## 6. Θυρακιθέτης σχιζμοειδής γραμμή (Shielded slot line or Fin line)

## 7. Ταινιογραμμή (Stripline)

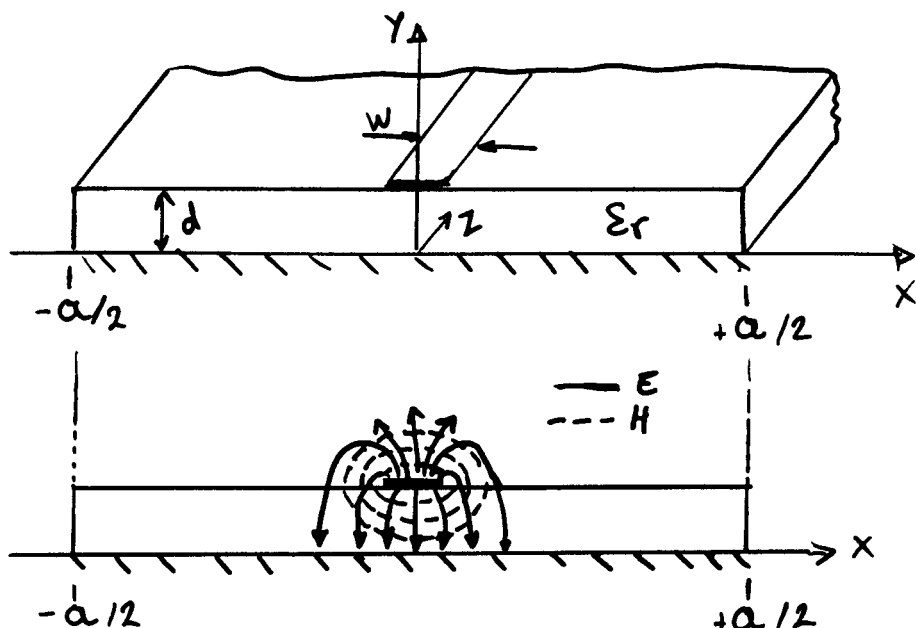
FIGURE 3.20

(a) Slot line; (b) shielded slot line or fin line; (c) stripline.



(c)

Μικροστανική Γραμμή - Λειτουργία σε ημι-TEM πυκνό<sup>(Pozar, σελ. 184)</sup>



Πυκνός ημι-TEM: Υπάρχουν μη-μηδενικές συντάσεις των ηλεκτρομαγνητικών πεδίων στη διεύθυνση διάδοσης, αλλά είναι πολύ ανθεντικές:  $E_z, H_z \ll$

Προβεγγιακή: Ηλεκτροστατική Νίγη

- Υποδειγμένη πυκνός TEM:  $E_z, H_z \sim 0$
- Υποδειγμένη ιδανικά ηλεκτρικά συχνάσματα στην θέση  $x = -\frac{a}{2}, +\frac{a}{2}$   
σε απόσταση πολύ μεγαλύτερη από το μήκος των υκονστρουκτών  $x = \pm a/2$ ,  $a \gg d$  για να μην διαταραχθούν το H/M πέδιο στα περιοριζόμενα γύρω από την μικροστανική γραμμή.

Πυκνός TEM: Διάδοση στην διεύθυνση -z:  $\bar{E}, \bar{H} \propto e^{-j\beta z}$

Εξισώσεις Laplace  $\bar{\nabla}_t^2 \Phi(x, y) = 0 \quad \text{για } |x| \leq a/2, 0 \leq y \leq d$

$$\nabla_t^2 = \frac{\partial^2}{\partial x^2} + \frac{\partial^2}{\partial y^2}$$

Οριακές Συνθήκες:

$$\Phi(x, y) \Big|_{\substack{x=\pm a/2}} = 0 \quad x = \pm a/2 \quad \text{Ιδανικά ηλεκτρικά συχνάσματα}$$

$$\Phi(x, y) \Big|_{\substack{y=0, d}} = 0 \quad y = 0 \quad \text{Επιστρέψιμη γειωσης} \\ y = d \quad \text{Συντήκη ακτινοβολίας.}$$

• Επίγειον με "χωρισμό μεταβλητών" και Εφαρμογή Ορικού Συνδικάτου  
 Περιοχή  $\Delta_{\text{η}} \cap \{y = d\}$   $\left\{ \begin{array}{l} \Phi(x, y) = \sum_{n=1,3,\dots}^{\infty} A_n \cos\left(\frac{n\pi x}{a}\right) \sinh\left(\frac{n\pi y}{a}\right) \\ 0 \leq y \leq d \end{array} \right.$

Περιοχή  $A \setminus \{y = d\}$   $\left\{ \begin{array}{l} \Phi(x, y) = \sum_{n=1,3,\dots}^{\infty} B_n \cos\left(\frac{n\pi x}{a}\right) e^{-n\pi y/a} \\ y > d \end{array} \right.$

• Συνδικάτη Συνέχειας στη διεπιφάνεια διηγεκτικού - αέρα:

$$\Phi(x, y) \Big|_{y=d^-} = \Phi(x, y) \Big|_{y=d^+} \rightarrow A_n \sinh\left(\frac{n\pi d}{a}\right) = B_n e^{-n\pi d/a}$$

• Ηγεκτικό ΤΙΕΔΙΟ

$$E_y = -\frac{\partial \Phi}{\partial y} = \begin{cases} -\sum_{n=1,3,\dots}^{\infty} A_n \cdot \left(\frac{n\pi}{a}\right) \cdot \cos\left(\frac{n\pi x}{a}\right) \cdot \cosh\left(\frac{n\pi y}{a}\right) \\ + \sum_{n=1,3,\dots}^{\infty} A_n \left(\frac{n\pi}{a}\right) \cdot \cos\left(\frac{n\pi x}{a}\right) \cdot \sinh\left(\frac{n\pi d}{a}\right) \cdot e^{-\frac{n\pi(y-d)}{a}} \end{cases}$$

• Επιφανειακή πλυκότητα φορτίου στην μικροτάτινη  $P_s(x, y=d)$

$$P_s = D_y(x, y=d^+) - D_y(x, y=d^-) = \varepsilon_0 E_y(x, y=d^+) - \varepsilon_0 \varepsilon_r E_y(x, y=d^-) =$$

$$(1) = \varepsilon_0 \sum_{n=1,3,\dots}^{\infty} A_n \left(\frac{n\pi}{a}\right) \cos\left(\frac{n\pi x}{a}\right) \cdot \left\{ \sinh\left(\frac{n\pi d}{a}\right) + \varepsilon_r \cosh\left(\frac{n\pi d}{a}\right) \right\}$$

↑ αντίληψη ότι δείχνει Fourier ως προς -x

• Προσεγγίση των  $P_s$  στην μικροτάτινη  $-w/2 \leq x \leq w/2$

$$(2) P_s = \begin{cases} 1 & \text{για } |x| < w/2 & \text{επιφάνεια μικροτάτινης} \\ 0 & \text{για } |x| > w/2 & \text{δι-επιφάνεια διηγεκτικού - αέρα.} \end{cases}$$

↳ Ομογενής (Κατα προσεγγίση) καταρροή υποδείξεως  $a \gg w$ .

• Θρόγγωντας τρυπομετρίες συνάρθεση:  $m, n = \text{ακέραιοι}$

$$(3) \int_0^{\pi} \cos(mx) \cos(nx) dx = \begin{cases} 0 & \text{για } m \neq n & 16 \times 9 \text{ είναι δίστιχη} \\ \frac{\pi}{2} & \text{για } m = n & \text{για } n \text{ μετάσημη} \end{cases}$$

• Εφικτώντας τις (1) και (2), πολλαπλασιάζοντας επι:  $\cos(n\pi x/a)$   
 και ορθογραντώντας από  $-a/2$  έως  $a/2$  Γιατίραψε:

$$A_n = \frac{4a \sin(n\pi w/2a)}{(n\pi)^2 \cdot \varepsilon_0 \cdot \left\{ \sinh(n\pi d/a) + \varepsilon_r \cosh(n\pi d/a) \right\}}$$

- Ταύτην ως προς το γειωμένο επίπεδο, σαν μέρος μικροτάσσιας:

$$V = - \int_0^d E_y(x=0, y) dy = \sum_{n=1,3,\dots}^{\infty} A_n \sinh\left(\frac{n\pi d}{a}\right)$$

- Όγκικό γραπτό στον μικροτάσσια

$$Q = \int_{-W/2}^{W/2} p_s(x) dx = W \quad \text{cb/m}$$

$\Rightarrow = 1$

- Στατική χωρητικότητα - ανα πολλά μικρά

$$C = \frac{Q}{V} = W / \sum_{n=1,3,\dots}^{\infty} A_n \sinh(n\pi d/a)$$

- Δρώσα Διπλεκτρική Σταθερά  $\epsilon_{r,eff}$

$$\epsilon_{r,eff} = \frac{C}{C_0} = \frac{\text{χωρητικότητα ανα πολ. μικρά } \epsilon_r \neq 1}{\text{χωρητικότητα ανα πολ. μικρά } \epsilon_r = 1}$$

Επίειδη: γενικά  $C = \epsilon_0 \epsilon_r \cdot \frac{\text{Επιφανεια πλακέων}}{\text{Αποστολή πλακών}}$

Και η διαφορά της  $\epsilon_{r,eff}$  από την  $\epsilon_r$  σφειδεύει ακριβείς σαν στη διπλεκτρική δεν πήρει σημασία το χωρό γύρω από την μικροτάσσια.

- Χαρακτηριστική Αντίσταση

$$Z_0 = \frac{1}{U_p \cdot C} = \frac{\sqrt{\epsilon_{r,eff}}}{C_{μετα} \cdot C}$$

Γραμμές Μετατόπασης.  $Z = R + j\omega L \approx j\omega L$

$$Y = G + j\omega C \approx j\omega C$$

$$\gamma = j\beta = \sqrt{Z \cdot Y}$$

$$Z_0 = \sqrt{\frac{Z}{Y}}$$

Ταυτότητα Φαίγκας

$$U_p = \frac{\omega}{\beta} = \frac{C_{μετα}}{\sqrt{\epsilon_{r,eff}}}$$

$$\beta = \omega \sqrt{\mu \epsilon_{r,eff}} = \frac{\omega}{C_{μετα}} \cdot \sqrt{\epsilon_{r,eff}} = K_0 \sqrt{\epsilon_{r,eff}}$$

- Σταθερά Εφασοδένσης  $a_c, a_d$  (Collin σελ. 155-156 & Pozar σελ. 188)

$$a_d = \frac{\pi}{\lambda_0} \frac{\epsilon_r}{\sqrt{\epsilon_{r,eff}}} \cdot \frac{\epsilon_{r,eff} - 1}{\epsilon_r - 1} \tan \delta \quad a_c \approx \frac{R_s}{Z_0} \frac{Neper}{m} \quad R_s = \sqrt{\frac{\omega \mu_0}{2 \sigma}}$$

## → Δρώσα Διηγεκτικής Σταθερά

1. Ημιστατ. και προσεγγίσεων (Pozar GEI. 185)

$$\varepsilon_{eff,1} \approx \frac{\varepsilon_r + 1}{2} + \frac{\varepsilon_r - 1}{2} \cdot \frac{1}{\sqrt{1 + 12 \cdot d/W}}$$

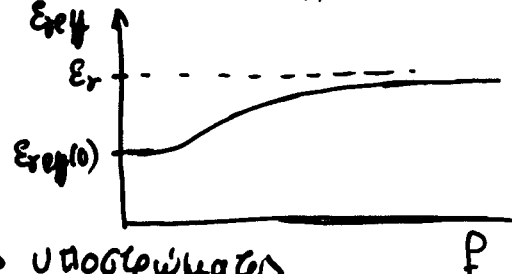
2. Βεγκέλιου ακρίβειας - Εκθεση Hammerstad: Collin GEI. 151.

$$\varepsilon_{eff}^{(0)} \approx \varepsilon_{eff,1} + F(\varepsilon_r, d) - 0.217 (\varepsilon_r - 1) \cdot \frac{T}{\sqrt{W \cdot d}}$$

$$F(\varepsilon_r, d) = \begin{cases} 0.02 (\varepsilon_r - 1) (1 - w/d)^2 & \text{jia } w/d < 1 \\ 0 & \text{jia } w/d \geq 1 \end{cases}$$

3. Εφαπτηγμένης  $\varepsilon_{eff}$  από την γυρνότητα Collin GEI. 162

$$\varepsilon_{eff}(f) = \varepsilon_r - \frac{\varepsilon_r - \varepsilon_{eff}(0)}{1 + (f/f_a)^m}$$



- Λεπτομερείς Collin GEI. 162
- Προγραμματικά: HP-App CAD

$T$  = παχούς χαλκού  $d = H$  = παχούς υποστρώματος

→ Χαρακτηριστική Aristicas

$$Z_0 = \begin{cases} \frac{60}{\sqrt{\varepsilon_{eff}}} \ln\left(\frac{8d}{W} + \frac{w}{4d}\right) & \text{jia } \frac{w}{d} \leq 1 \\ \frac{120\pi}{\sqrt{\varepsilon_{eff}}^2 \left[ W/d + 1.393 + 0.667 \ln(W/d + 1.444) \right]} & \text{jia } \frac{w}{d} \geq 1 \end{cases}$$

→ Υπολογισμός πλαίσιου γραμμής  $w/d = ?$

jia δεδομένη  $Z_0$  kai  $\varepsilon_r$

$$\frac{w}{d} = \begin{cases} 8e^A / (e^{2A} - 2) & \text{jia } w/d < 2 \\ \frac{2}{\pi} \left\{ B - 1 - \ln(2B - 1) + \frac{\varepsilon_r - 1}{2\varepsilon_r} \left[ \ln(B - 1) + 0.39 - \frac{0.61}{\varepsilon_r} \right] \right\} & \text{jia } w/d > 2 \end{cases}$$

Όπου:

$$A = \frac{Z_0}{60} \sqrt{\frac{\varepsilon_r + 1}{2}} + \frac{\varepsilon_r - 1}{\varepsilon_r + 1} \left( 0.23 + \frac{0.11}{\varepsilon_r} \right)$$

$$B = \frac{\eta_0 \cdot \pi}{2Z_0 \sqrt{\varepsilon_r}} = \frac{377 \cdot \pi}{2Z_0 \sqrt{\varepsilon_r}}$$

# Ρευματική Ηλεκτρονίκη Μικροσύντομης Γράφησης

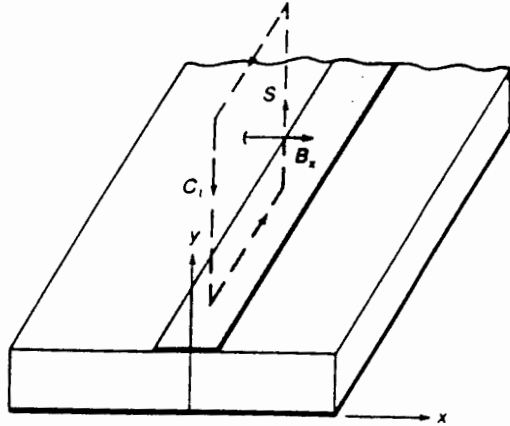


FIGURE 3.21  
Surface used to find the magnetic flux linkage in a microstrip line.

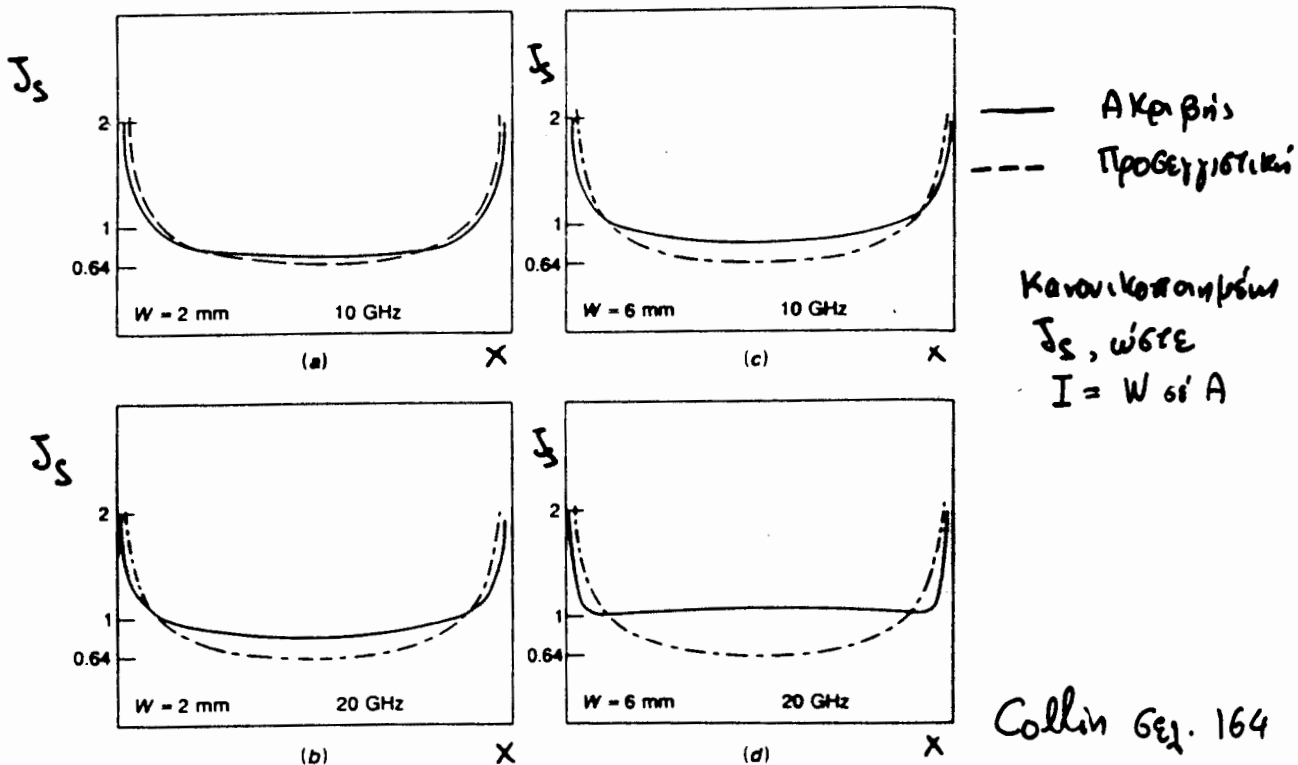
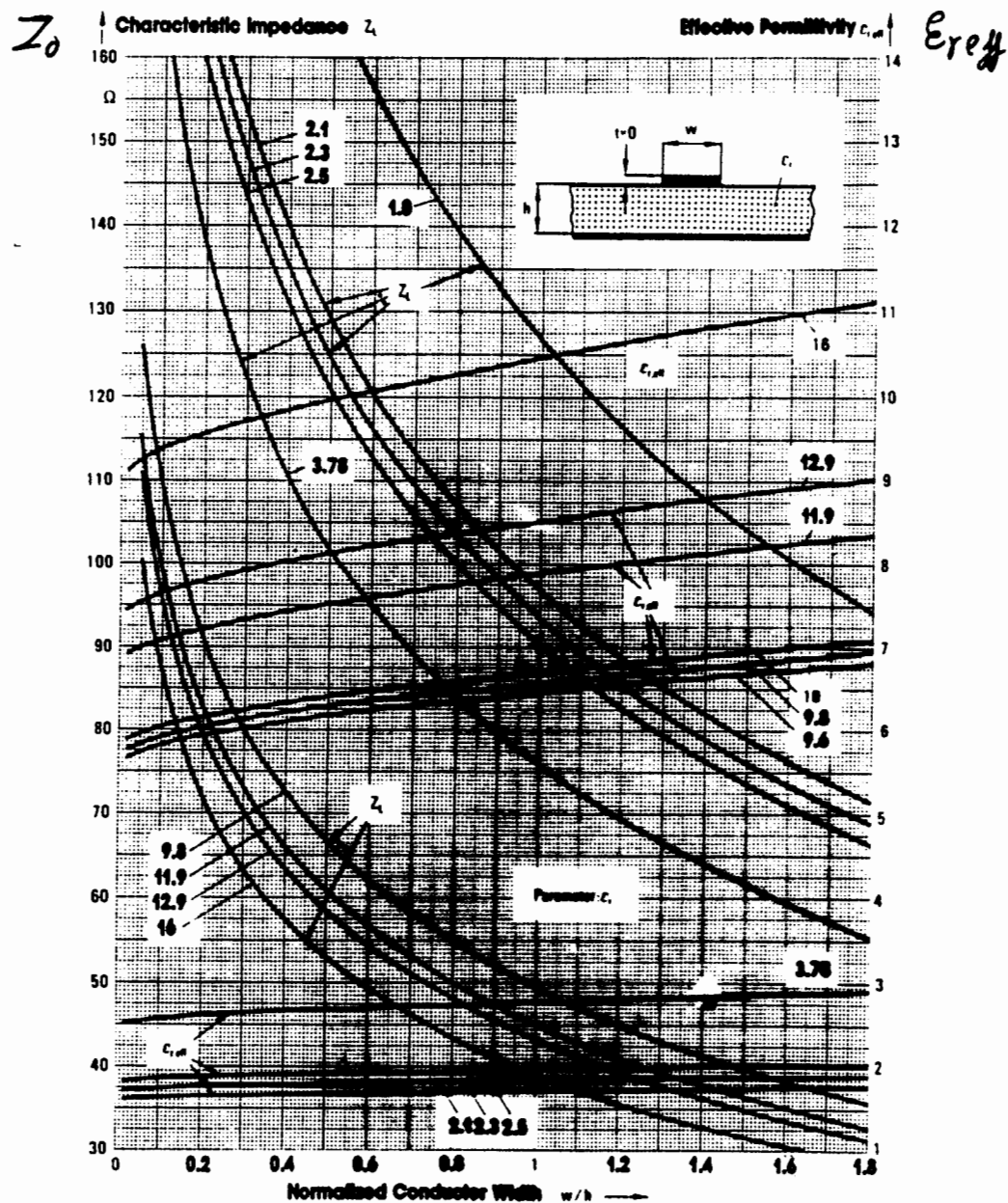


FIGURE 3.29  
Current distribution on the microstrip for an alumina substrate with  $H = 1 \text{ mm}$  and two different widths. The broken curves give the quasistatic distribution. (a)  $W = 2 \text{ mm}$ ,  $f = 10 \text{ GHz}$ ; (b)  $W = 2 \text{ mm}$ ,  $f = 20 \text{ GHz}$ ; (c)  $W = 6 \text{ mm}$ ,  $f = 10 \text{ GHz}$ ; (d)  $W = 6 \text{ mm}$ ,  $f = 20 \text{ GHz}$ .

- Προσέγγιστική ρευματική ηλεκτρονίκη από τον "Επίπεδο Απεικόνισης"  

$$J_s(x) \approx \frac{2Q}{\pi \cdot W \sqrt{1 - x^2 / (W/2)^2}}$$
(Collin Ex. 16)
- Ακριβής Ρευματική ηλεκτρονίκη

Χαρακτηριστική Αντίσταση και Δρώση Διγέλιθου Στρωμάτος - 1  
Μικροταινιακών Τραβών



**Fig. 3.4** Circuit parameters  $Z_L$  and  $\epsilon_{r,eff}$  of microstrip on various technologically important substrates: PTFE ( $\epsilon_r = 2.1$ ), polyolefin ( $\epsilon_r = 2.3$ ), glass-reinforced PTFE ( $\epsilon_r = 2.5$ ), fused quartz ( $\epsilon_r = 3.78$ ), alumina ceramic ( $\epsilon_r = 9.6$ , 9.8, or 10), semi-insulating Si ( $\epsilon_r = 11.9$ ), semi-insulating GaAs ( $\epsilon_r = 12.9$ ), and nonmagnetic ferrite ( $\epsilon_r = 16$ ), with  $t = 0$  for  $w/h \leq 1.8$  by the method of lines.

Χαρακτηριστική Αντίσταση και Δυναμική Διελεκτρική Σταθερά - 2

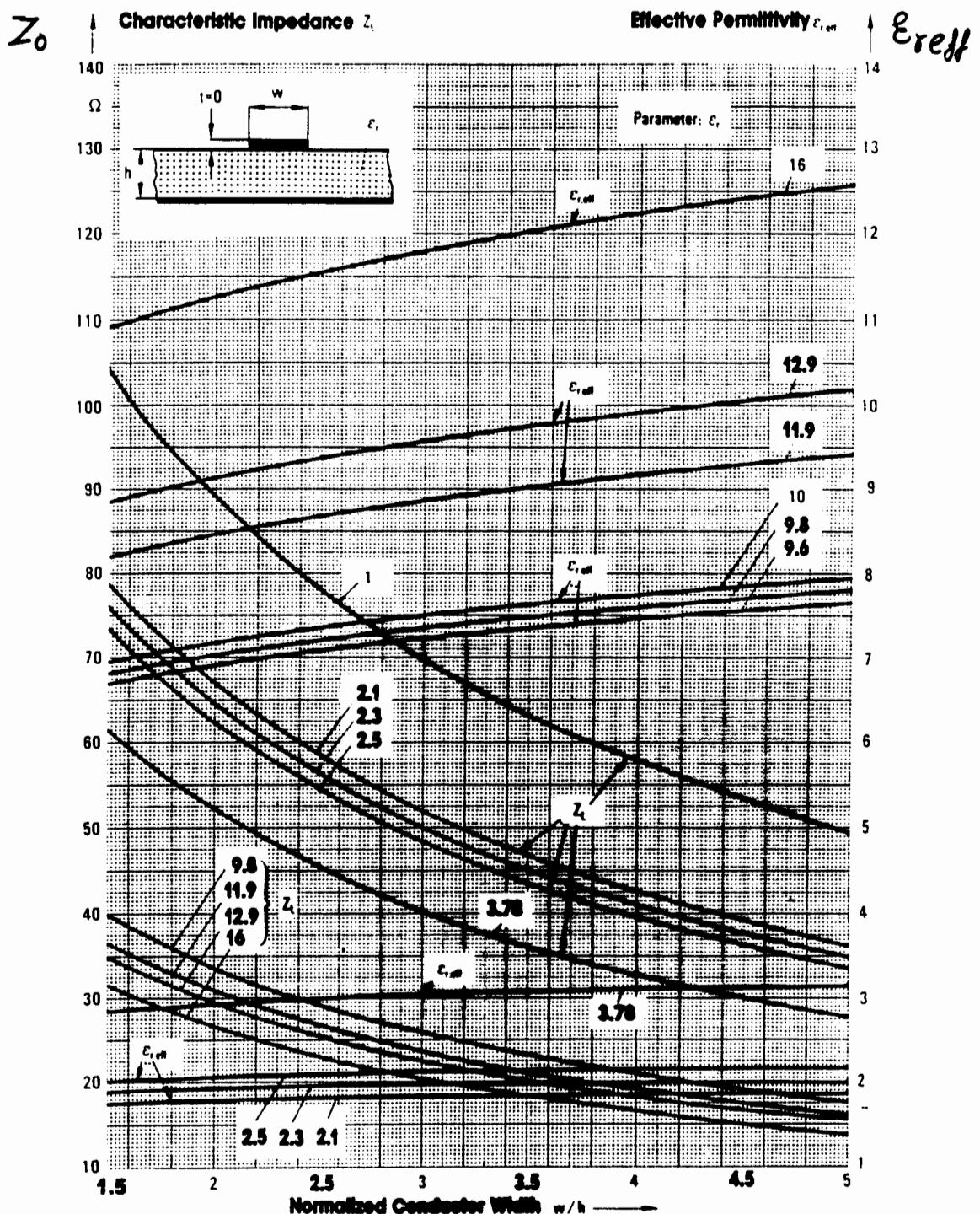


**Fig. 3.5** Continuation of Figure 3.4 for larger conductor width  $1.5 \leq w/h \leq 5$ .

# Xapaximpen671'ni Avrictor Van Apwia Dmleupilen' Etawipai - 3

**Table 3.1** Calculated circuit parameters  $Z_{L0}$  and  $\epsilon_{r,eff}$  as shown in Figures 3.4 and 3.5, using static variation of the method of lines [2.86, 2.89, 3.99, 3.100].

w/h	$Z_{L0}$ in $\Omega$	Effective Permittivity $\epsilon_{r,eff}$ for $\epsilon_r =$									
		2.1	2.3	2.5	3.78	9.6	9.8	10.0	11.9	12.9	16
0.02	359.45	1.604	1.713	1.822	2.517	5.665	5.774	5.882	6.909	7.450	9.125
0.03	335.25	1.608	1.718	1.827	2.526	5.692	5.803	5.911	6.945	7.488	9.173
0.04	318.05	1.611	1.722	1.832	2.534	5.714	5.826	5.935	6.973	7.519	9.212
0.05	304.64	1.614	1.725	1.835	2.540	5.731	5.846	5.956	6.997	7.546	9.245
0.1	263.23	1.625	1.738	1.850	2.567	5.808	5.926	6.037	7.096	7.653	9.380
0.15	238.62	1.634	1.748	1.861	2.587	5.873	5.986	6.099	7.170	7.734	9.482
0.2	221.62	1.640	1.756	1.870	2.604	5.923	6.036	6.150	7.232	7.802	9.567
0.3	197.21	1.652	1.769	1.886	2.632	6.008	6.124	6.239	7.340	7.919	9.714
0.4	180.21	1.662	1.781	1.900	2.657	6.083	6.201	6.318	7.435	8.023	9.845
0.6	156.09	1.680	1.802	1.924	2.701	6.215	6.336	6.457	7.602	8.205	10.074
0.8	139.25	1.695	1.820	1.945	2.740	6.334	6.457	6.580	7.752	8.369	10.280
1.0	126.58	1.710	1.838	1.965	2.777	6.448	6.574	6.700	7.897	8.527	10.479
1.2	116.30	1.723	1.853	1.983	2.810	6.549	6.677	6.806	8.025	8.666	10.654
1.4	107.84	1.735	1.868	1.999	2.840	6.644	6.774	6.905	8.145	8.797	10.819
1.6	100.62	1.747	1.881	2.015	2.868	6.731	6.864	6.996	8.255	8.918	10.972
1.8	94.39	1.757	1.893	2.029	2.895	6.807	6.948	7.082	8.359	9.032	11.115
2.0	89.06	1.767	1.904	2.042	2.920	6.890	7.027	7.163	8.458	9.139	11.251
2.5	78.13	1.788	1.930	2.072	2.975	7.063	7.204	7.344	8.677	9.379	11.553
3.0	69.77	1.807	1.953	2.097	3.023	7.213	7.357	7.501	8.867	9.586	11.815
3.5	63.12	1.823	1.971	2.119	3.064	7.343	7.490	7.637	9.032	9.767	12.043
4.0	57.69	1.837	1.988	2.139	3.100	7.457	7.607	7.757	9.178	9.925	12.243
5.0	49.33	1.861	2.016	2.171	3.161	7.649	7.804	7.958	9.421	10.192	12.580
10.0	28.97	1.929	2.098	2.266	3.340	8.214	8.382	8.549	10.140	10.977	13.571

## Συγχρέες Μικροταινιακές Γραμμές

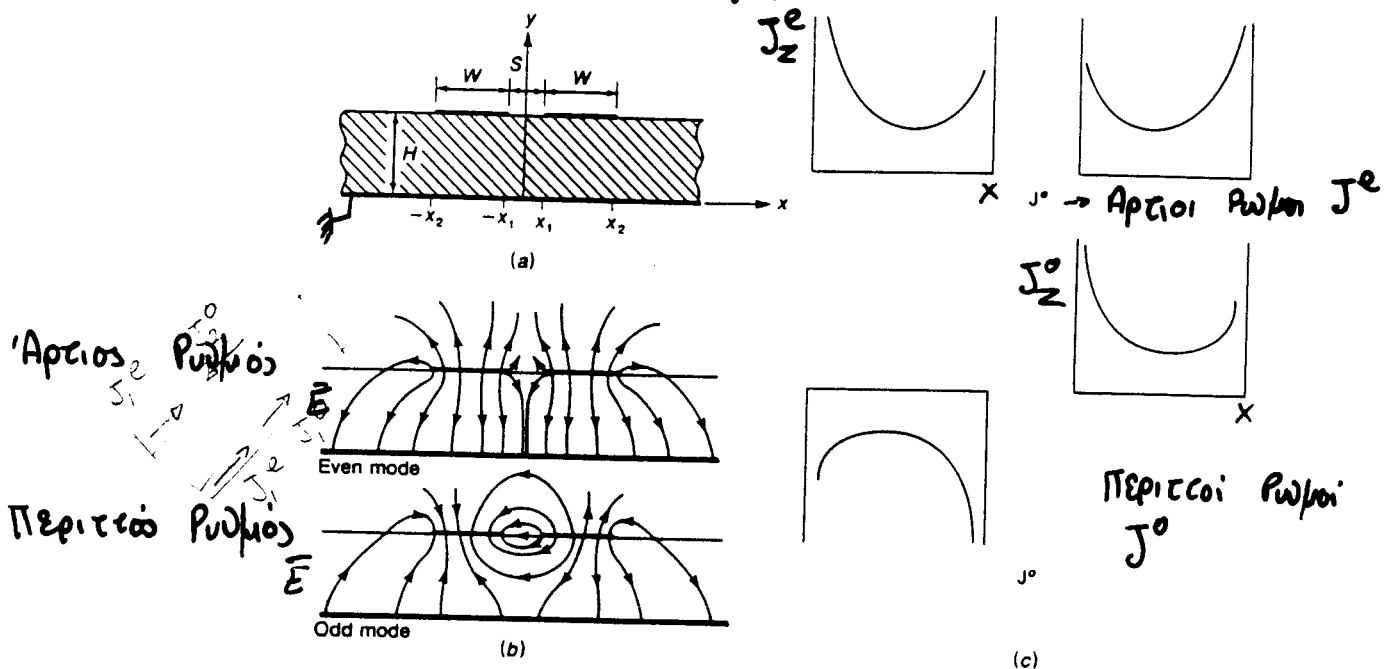


FIGURE 3.30

(a) Coupled microstrip line; (b) the electric field distribution for the even and odd modes; (c) the current distribution for the even and odd modes.

Collin Eq. 16S

Διεγειρόμενα Ρυθμοί : Σε μια γραμμή 3-σημείων διεγειρούνται γενικά δύο τύποι ρυθμών TEM.

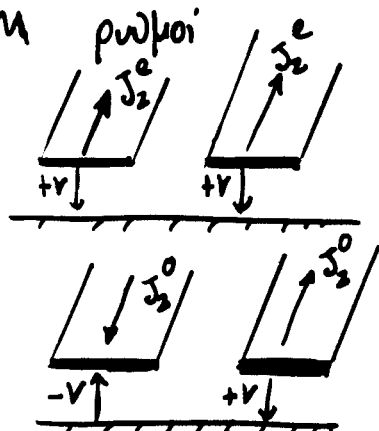
Συγχρέες Μικροταινιακές γραμμές : Διεγειρούνται δύο ημι-TEM ρυθμούς

Aptios ημι-TEM ρυθμούς (even mode) :

↳ Οι αριθμοί δύο μικροταινιακές γραμμές βρίσκονται στο ίδιο συντελεστικό  $+V, +V$

Περισσοίς ημι-TEM ρυθμούς (odd mode)

↳ Οι αριθμοί δύο μικροταινιακές γραμμές βρίσκονται σε αντίθετα συντελεστικά  $-V, +V$



### Ρευματική Καταροφή

- Οι αριθμοί δύο μικροταινιακές γραμμές στην αέρα - ανούσια διηλεκτρικά υλοστρατικά και αποδίδουν γειωση:

$$\text{Απτιοί ρυθμοί : } J_z^e(x) = \frac{x}{\sqrt{(x^2 - x_1^2)(x_2^2 - x^2)}}$$

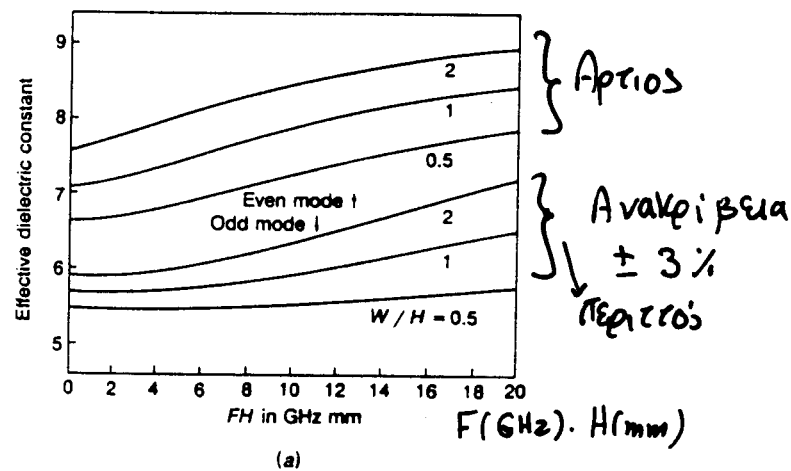
$$\text{Περισσοίς ρυθμοί } J_z^o(x) = \frac{x_2}{\sqrt{(x^2 - x_1^2)(x_2^2 - x^2)}}$$

- Η απονέκκεια στις ακτίδες είναι της μορφής  $\propto 1/x$

# Δρώγα Διηγεκτίκη Σειράς Αριού και Περικού Ρυθμού

$$S/H = 0.25$$

$$\epsilon_r = 9.7 \quad (\text{Al}_2\text{O}_3)$$



Ανακρίβεια  $\pm 8\%$

$$Z_0^0, Z_0^e$$

Ανακρίβεια  $\pm 3\%$

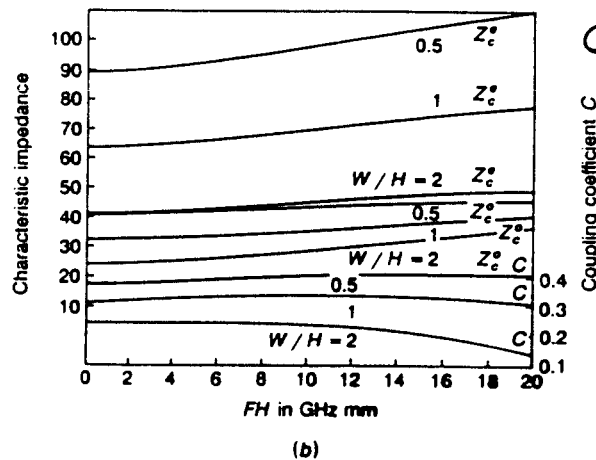


FIGURE 3.31

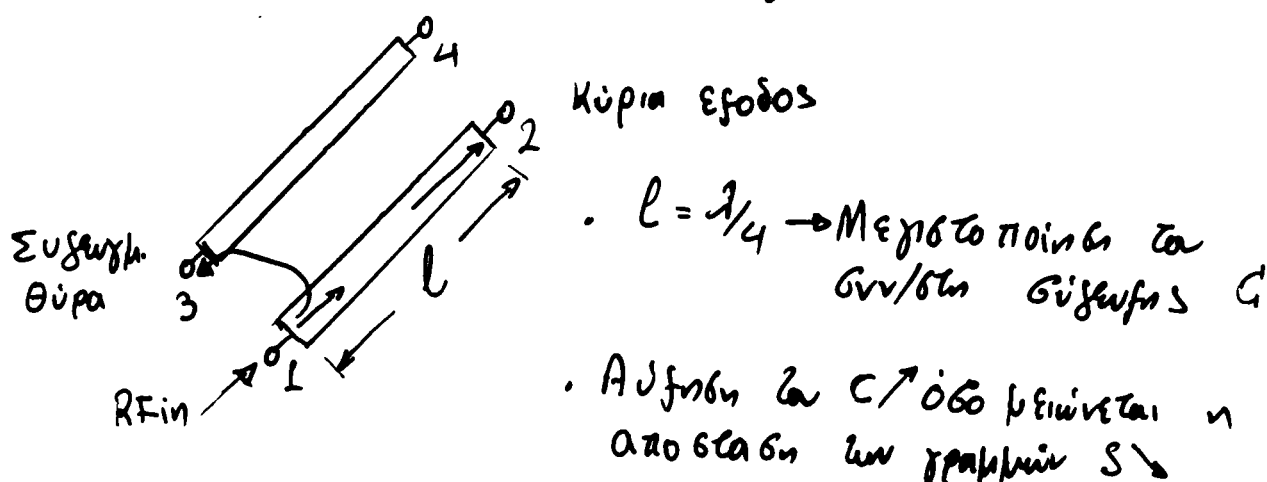
Dispersion characteristics of a coupled microstrip line on an alumina substrate.  $S/H = 0.25$ ,  $\epsilon_r = 9.7$ . (a) Even- and odd-mode effective dielectric constant; (b) even- and odd-mode characteristic impedance and coupling coefficient  $C$ .

$$\text{Συντελεστής Σύγενης } C = \frac{Z_0^e - Z_0^0}{Z_0^e + Z_0^0} = \frac{1 - (Z_0^0/Z_0^e)}{1 + (Z_0^0/Z_0^e)}$$

↳ Επιτελεστήρια τύπος με πολ. 2.5 : 1 σε 8 dB.

$$C(\text{dB}) = 20 \log(C)$$

Αποκοντίσμα Θύρα



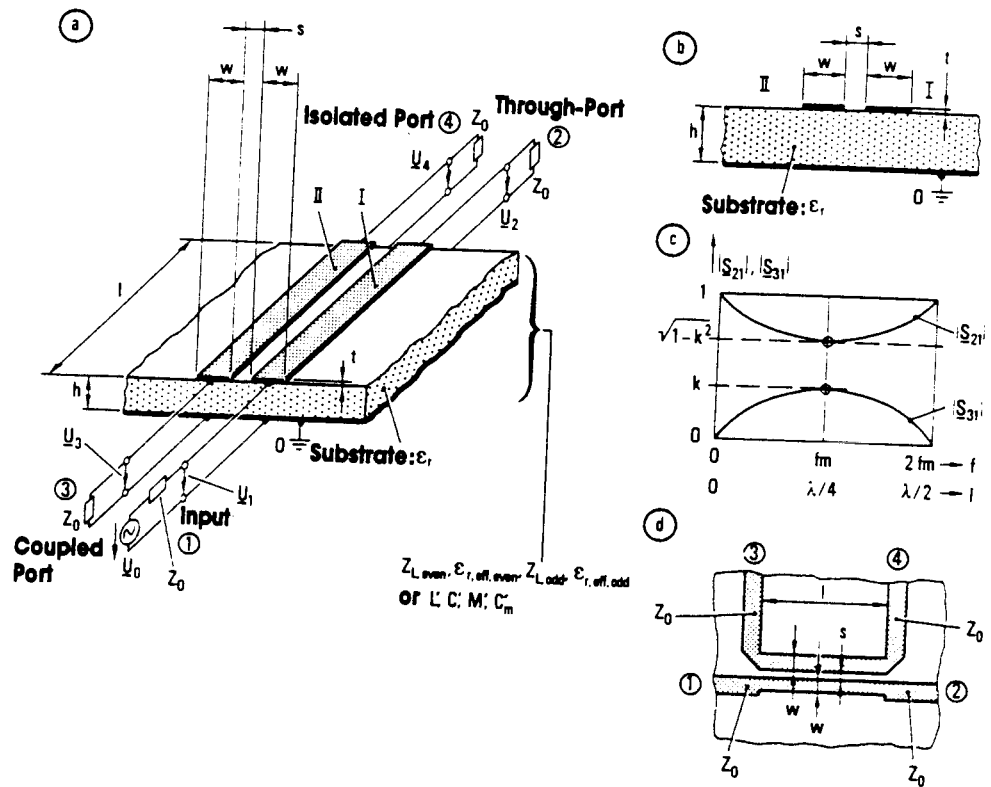


**Fig. 9.1** Symmetric microstrip coupled section: (a) schematic diagram; (b) circuit cross section; (c) principal transmission characteristics (ideal TEM coupler); (d) actual circuit.

# Συγερμένες Ταινιογράμμες (Coupled Strip Lines)

Collin Ch. 170-174

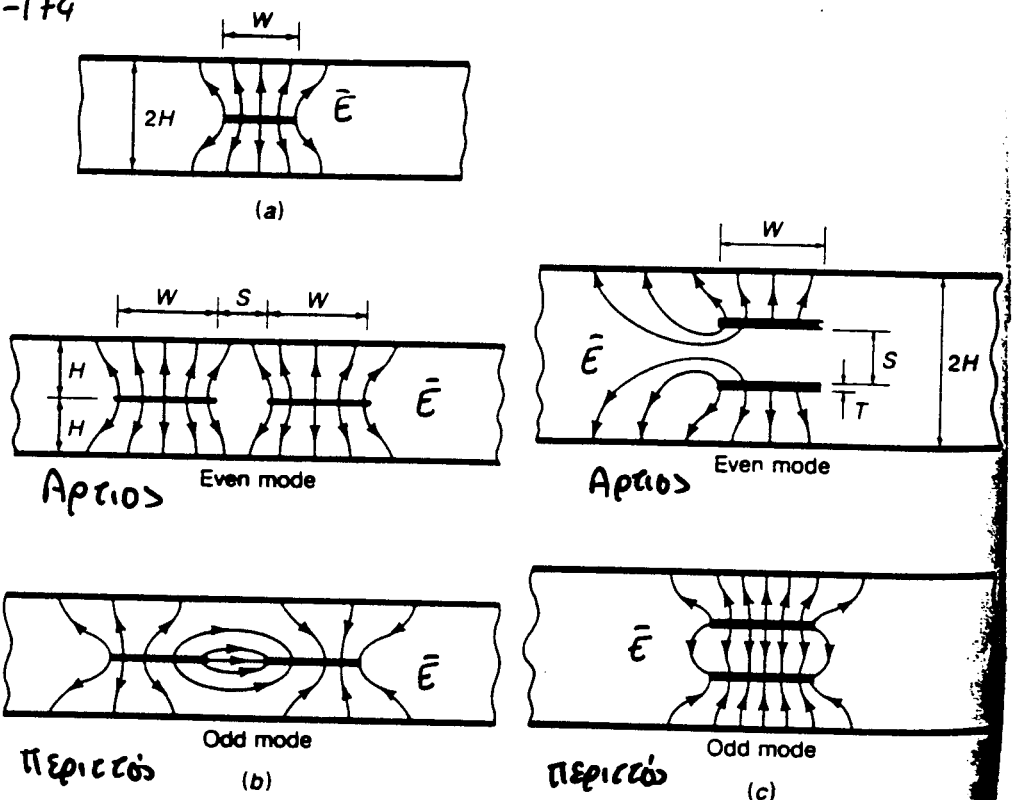
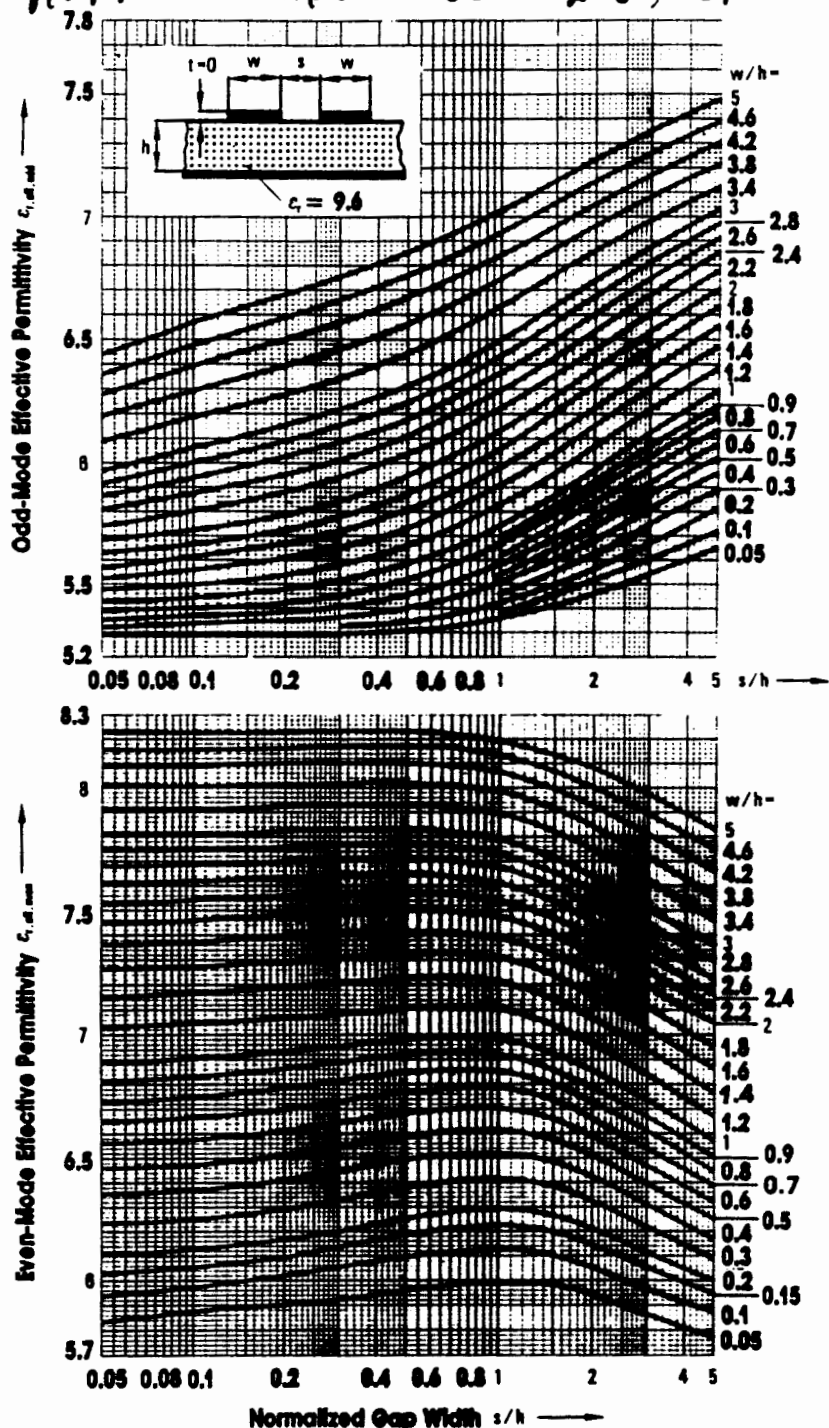


FIGURE 3.34

(a) The basic strip-line configuration; (b) coupled strip line using coplanar strips; (c) coupled strip line using broadside coupled strips. The electric field lines for the TEM modes are shown.

- Οι διεγειρόμενοι ρυθμοί είναι καταρτικοί TEM
- Οι γυντελεστικοί εγγράφοι είναι μεγαλύτερος από αυτούς των μηδιοταντάκων γραμμών C (Υπολογισμοί : Collin Ch. 173)

Характеристики Активных и Активно-Симметрических Структур - 1  
Микротранзисторы на основе транспонторов GE Al<sub>2</sub>O<sub>3</sub>,  $\epsilon_r \approx 9.6$



**Fig. 9.4** Effective even and odd mode permittivities  $\epsilon_{r,eff,even}$  and  $\epsilon_{r,eff,odd}$  of coupled microstrip lines on Al<sub>2</sub>O<sub>3</sub> substrate ( $\epsilon_r = 9.6$ ) from static analysis with the Green's functions method [2.77, 2.80].

Հարակումը Արտիգան և Դանիա Տիշչելիք Ելեկտրոն - 2  
Գյուղական լիկուատուր յափառ լամպեր 6E Al<sub>2</sub>O<sub>3</sub>,  $\epsilon_r = 9.6$

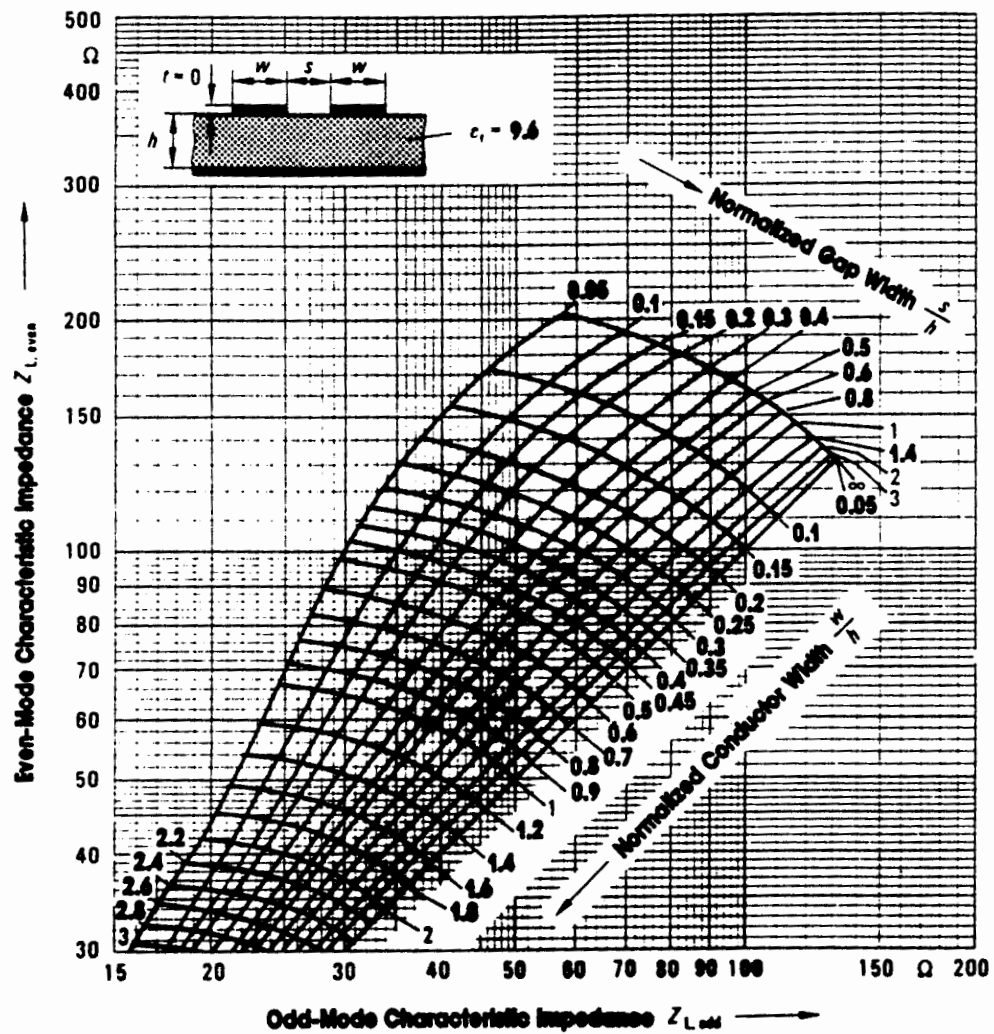


**Fig. 9.3** Even and odd mode characteristic impedances  $Z_{L,even}$  and  $Z_{L,odd}$  of coupled microstrip lines on Al<sub>2</sub>O<sub>3</sub> ceramic substrate ( $\epsilon_r = 9.6$ ) from static analysis with the Green's functions method [2.77, 2.80].

**Δρώσα Διπλεκτρική Σταθερά Εγενήθηκεν Μικροστρίπειν  
Γραμμήν Τυπωθείσαν εε  $\text{Al}_2\text{O}_3$ ,  $\epsilon_r = 9.8$**

**Table 9.2 Even and odd mode effective permittivities  $\epsilon_{r,\text{eff,even}}$ , and  $\epsilon_{r,\text{eff,odd}}$  for coupled microstrip lines on  $\text{Al}_2\text{O}_3$  ceramic substrates ( $\epsilon_r = 9.8$ ) for a conductor thickness  $t = 0$  from the variational method [2.46, 3.32] for the quasistatic case  $h/\lambda_0 = 10^{-5}$ .**

**Aptios Ρυθμός**

w/h	Even-Mode Effective Permittivity $\epsilon_{r,\text{eff,even}}$ for $s/h =$														
	0.05	0.1	0.2	0.4	0.6	0.8	1	1.2	1.4	1.6	1.8	2	2.5	3	4
0.4	6.491	6.516	6.558	6.620	6.656	6.672	6.673	6.662	6.644	6.621	6.594	6.567	6.501	6.444	6.361
0.6	6.705	6.726	6.764	6.818	6.849	6.860	6.856	6.841	6.819	6.793	6.763	6.733	6.661	6.599	6.509
0.8	6.891	6.910	6.943	6.989	7.014	7.020	7.012	6.994	6.969	6.939	6.908	6.876	6.800	6.735	6.640
1	7.054	7.071	7.100	7.140	7.159	7.161	7.149	7.128	7.101	7.069	7.036	7.003	6.924	6.857	6.760
1.2	7.199	7.214	7.239	7.273	7.288	7.286	7.271	7.248	7.219	7.186	7.152	7.118	7.037	6.969	6.870
1.4	7.328	7.342	7.364	7.393	7.403	7.398	7.382	7.357	7.327	7.293	7.258	7.223	7.142	7.073	6.973
1.6	7.444	7.456	7.476	7.500	7.507	7.500	7.482	7.456	7.425	7.391	7.356	7.320	7.238	7.169	7.069
1.8	7.549	7.560	7.577	7.598	7.602	7.593	7.574	7.547	7.516	7.481	7.446	7.410	7.328	7.259	7.159
2	7.643	7.653	7.669	7.687	7.689	7.679	7.658	7.631	7.599	7.565	7.529	7.494	7.412	7.344	7.244
2.5	7.844	7.853	7.865	7.877	7.876	7.863	7.842	7.814	7.782	7.748	7.714	7.679	7.600	7.533	7.435
3	8.007	8.014	8.024	8.033	8.029	8.016	7.994	7.967	7.936	7.903	7.870	7.837	7.760	7.695	7.600
3.5	8.142	8.148	8.156	8.163	8.158	8.144	8.122	8.096	8.067	8.035	8.003	7.972	7.898	7.836	7.741

**Περιεχόμενος**

**Table 9.2 (cont'd)**

w/h	Odd-Mode Effective Permittivity $\epsilon_{r,\text{eff,odd}}$ for $s/h =$														
	0.05	0.1	0.2	0.4	0.6	0.8	1	1.2	1.4	1.6	1.8	2	2.5	3	4
0.4	5.428	5.439	5.457	5.495	5.535	5.577	5.620	5.661	5.702	5.740	5.777	5.810	5.883	5.941	6.022
0.6	5.458	5.474	5.501	5.552	5.603	5.653	5.702	5.750	5.795	5.838	5.877	5.914	5.992	6.054	6.139
0.8	5.496	5.519	5.554	5.617	5.676	5.733	5.788	5.840	5.889	5.934	5.976	6.014	6.095	6.159	6.247
1	5.542	5.571	5.615	5.687	5.754	5.817	5.875	5.931	5.982	6.029	6.072	6.111	6.194	6.259	6.348
1.2	5.594	5.630	5.681	5.762	5.834	5.901	5.963	6.020	6.073	6.121	6.165	6.205	6.289	6.354	6.444
1.4	5.650	5.693	5.750	5.839	5.916	5.986	6.050	6.109	6.163	6.212	6.256	6.296	6.380	6.445	6.535
1.6	5.708	5.758	5.822	5.916	5.997	6.069	6.135	6.195	6.249	6.299	6.344	6.384	6.468	6.532	6.622
1.8	5.768	5.825	5.894	5.994	6.077	6.151	6.218	6.279	6.334	6.383	6.428	6.468	6.552	6.616	6.704
2	5.829	5.893	5.967	6.071	6.156	6.231	6.299	6.360	6.415	6.464	6.509	6.549	6.632	6.695	6.783
2.5	5.980	6.060	6.146	6.257	6.345	6.421	6.489	6.550	6.604	6.653	6.697	6.736	6.816	6.878	6.964
3	6.125	6.219	6.314	6.430	6.519	6.594	6.662	6.722	6.775	6.823	6.866	6.904	6.982	7.041	7.125
3.5	6.260	6.368	6.471	6.589	6.677	6.752	6.818	6.877	6.929	6.976	7.017	7.054	7.130	7.187	7.269

*Характеристики Активации и Активации Генера  
Симметрических и несимметрических гравитационных полей на Al<sub>2</sub>O<sub>3</sub>*

Table 9.1 Even and odd mode characteristic impedances  $Z_{L,\text{even}}$  and  $Z_{L,\text{odd}}$  of coupled microstrip lines on Al<sub>2</sub>O<sub>3</sub> ceramic substrate ( $\epsilon_r = 9.8$ ) for conductor thickness  $t = 0$  from the variational method [2.46, 3.32] for the quasistatic case  $h/\lambda_0 = 10^{-5}$ .

*Активации Пулюс*

w/h	Even-Mode Characteristic Impedance $Z_{L,\text{even}}$ in $\Omega$ for $s/h = \frac{1}{2}$														
	0.05	0.1	0.2	0.4	0.6	0.8	1	1.2	1.4	1.6	1.8	2	2.5	3	4
0.4	106.75	104.22	99.89	93.41	88.81	85.44	82.92	81.02	79.58	78.48	77.63	76.98	75.92	75.33	74.75
0.6	88.09	86.40	83.43	78.77	75.32	72.74	70.78	69.28	68.14	67.27	66.60	66.08	65.24	64.78	64.32
0.8	75.44	74.22	72.03	68.50	65.83	63.79	62.22	61.02	60.10	59.39	58.84	58.43	57.75	57.38	57.02
1	66.17	65.23	63.54	60.77	58.64	56.99	55.71	54.73	53.97	53.39	52.94	52.60	53.05	51.75	51.47
1.2	59.03	58.29	56.94	54.71	52.96	51.60	50.54	49.72	49.09	48.60	48.23	47.95	47.50	47.26	47.03
1.4	53.34	52.74	51.64	49.80	48.34	47.20	46.31	45.61	45.08	44.67	44.35	44.12	43.75	43.55	43.37
1.6	48.69	48.19	47.27	45.73	44.50	43.53	42.76	42.17	41.71	41.36	41.09	40.90	40.59	40.43	40.28
1.8	44.81	44.39	43.62	42.30	41.24	40.40	39.73	39.23	38.83	38.53	38.31	38.14	37.88	37.75	37.63
2	41.52	41.16	40.50	39.36	38.44	37.71	37.14	36.69	36.35	36.09	35.89	35.75	35.53	35.43	35.33
2.5	35.13	34.88	34.40	33.58	32.91	32.37	31.95	31.62	31.37	31.18	31.04	30.94	30.81	30.75	30.69
3	30.48	30.29	29.93	29.31	28.80	28.38	28.06	27.81	27.62	27.48	27.38	27.31	27.22	27.19	27.14
3.5	26.93	26.79	26.51	26.02	25.61	25.29	25.03	24.83	24.68	24.58	24.50	24.45	24.39	24.37	24.55

*Таблицы* **Пулюс**

Table 9.1 (cont'd)

w/h	Odd-Mode Characteristic Impedance $Z_{L,\text{odd}}$ in $\Omega$ for $s/h = \frac{1}{2}$														
	0.05	0.1	0.2	0.4	0.6	0.8	1	1.2	1.4	1.6	1.8	2	2.5	3	4
0.4	29.93	35.12	41.72	49.87	55.12	58.85	61.61	63.72	65.37	66.67	67.72	68.57	70.10	71.09	72.21
0.6	26.88	31.22	36.66	43.34	47.63	50.69	52.96	54.71	56.07	57.16	58.05	58.77	60.11	60.98	62.00
0.8	24.86	28.66	33.32	38.98	42.59	45.15	47.06	48.53	49.69	50.62	51.38	52.01	53.18	53.96	54.89
1	23.35	26.74	30.83	35.71	38.80	40.99	42.63	43.88	44.88	45.68	46.35	46.90	47.94	48.65	49.50
1.2	22.14	25.19	28.82	33.10	35.79	37.69	39.10	40.19	41.06	41.77	42.35	42.84	43.77	44.42	45.20
1.4	21.11	23.89	27.15	30.94	33.30	34.96	36.20	37.16	37.93	38.55	39.07	39.51	40.36	40.95	41.67
1.6	20.22	22.76	25.71	29.10	31.19	32.66	33.76	34.61	35.29	35.85	36.15	36.71	37.48	38.02	38.70
1.8	19.42	21.75	24.44	27.49	29.37	30.68	31.66	32.42	33.04	33.53	33.96	34.32	35.02	35.52	36.15
2	18.70	20.86	23.32	26.08	27.77	28.95	29.85	30.51	31.07	31.52	31.91	32.24	32.89	33.36	33.94
2.5	17.15	18.96	20.97	23.18	24.51	25.44	26.13	26.67	27.11	27.48	27.79	28.06	28.60	29.00	29.49
3	15.87	17.41	19.10	20.92	21.99	22.74	23.30	23.74	24.10	24.41	24.67	24.90	25.35	25.69	26.09
3.5	14.79	16.12	17.56	19.08	19.97	20.59	21.05	21.42	21.72	21.98	22.20	22.40	22.78	23.07	23.39

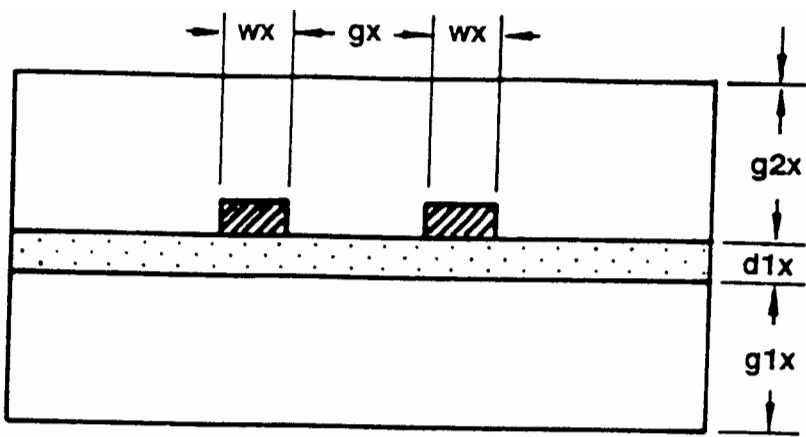


Figure 11. Suspended substrate coupled lines.

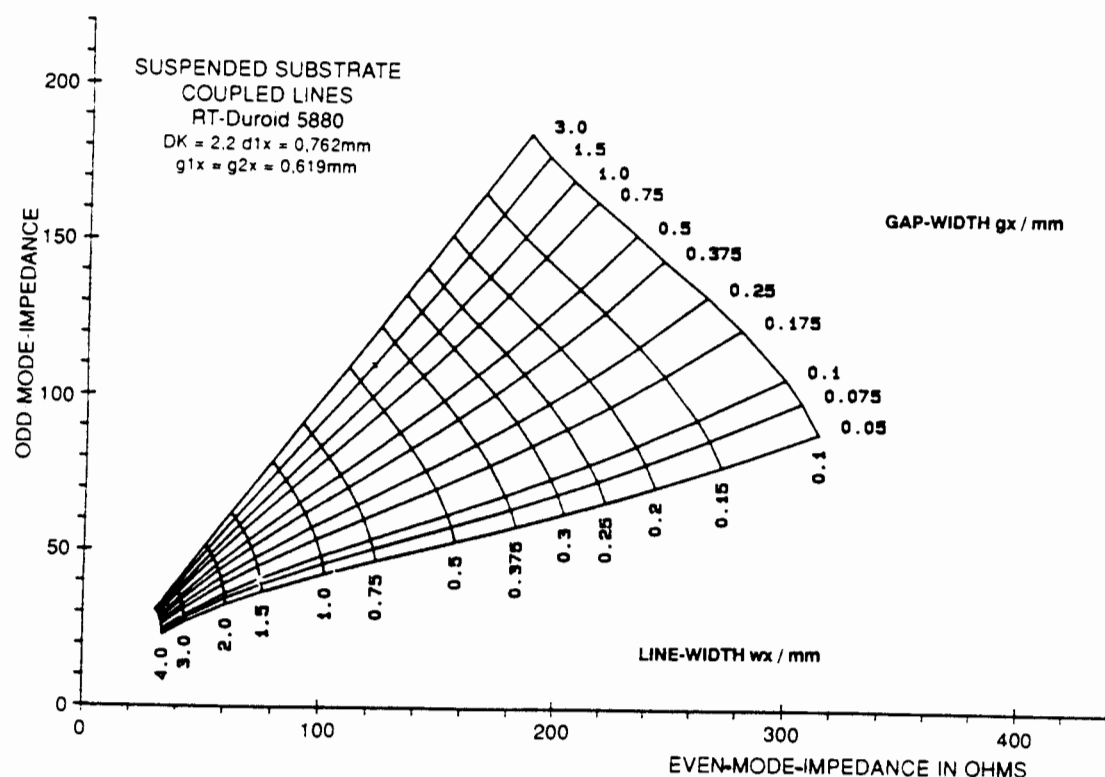


Figure 13. Even- and odd-mode impedances of suspended substrate coupled lines (substrate, RT 5880).

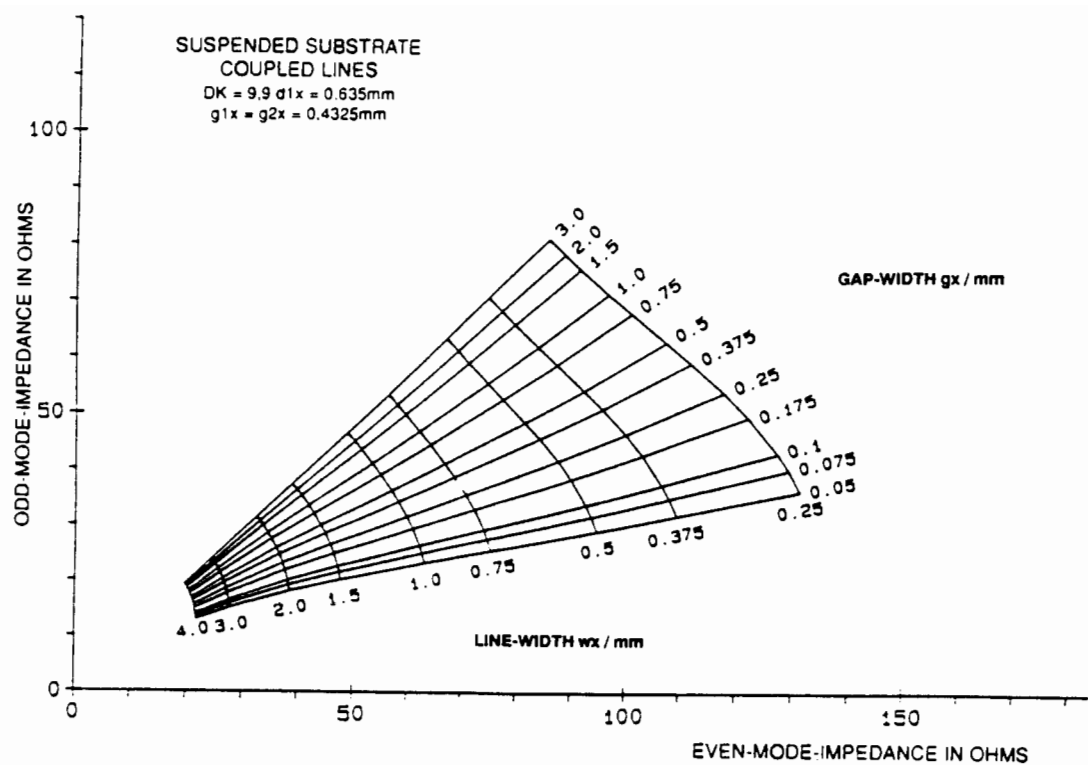


Figure 14. Even- and odd-mode, impecances of suspended substrate coupled lines (substrate. AL203).

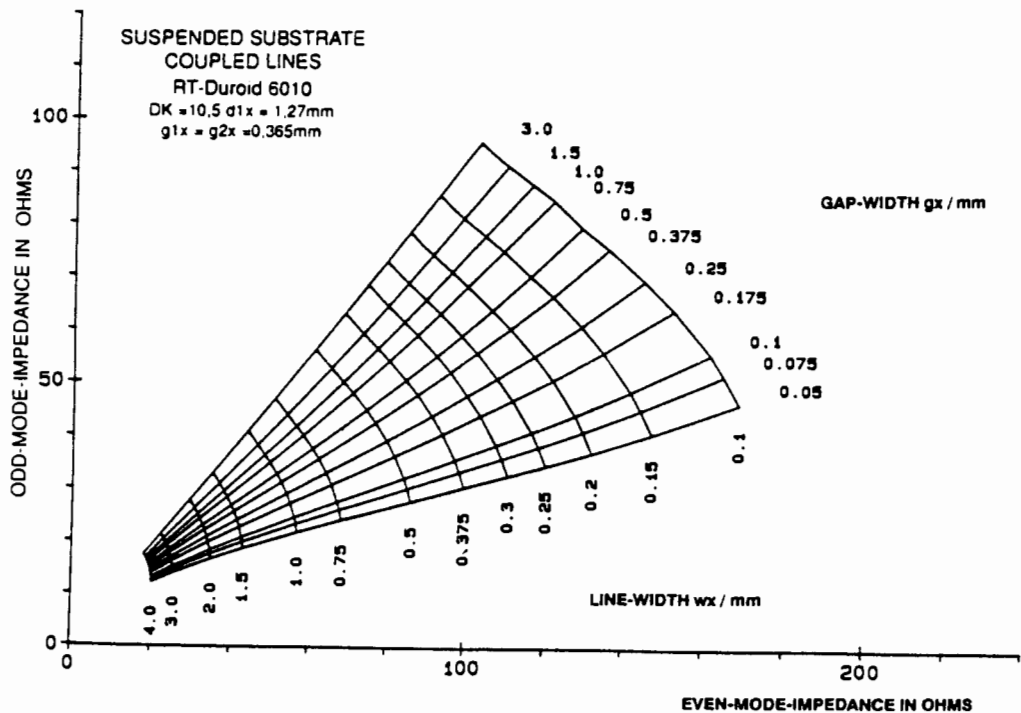


Figure 15. Even- and odd-mode impedances of suspended substrate coupled lines (substrate, RT 6010).

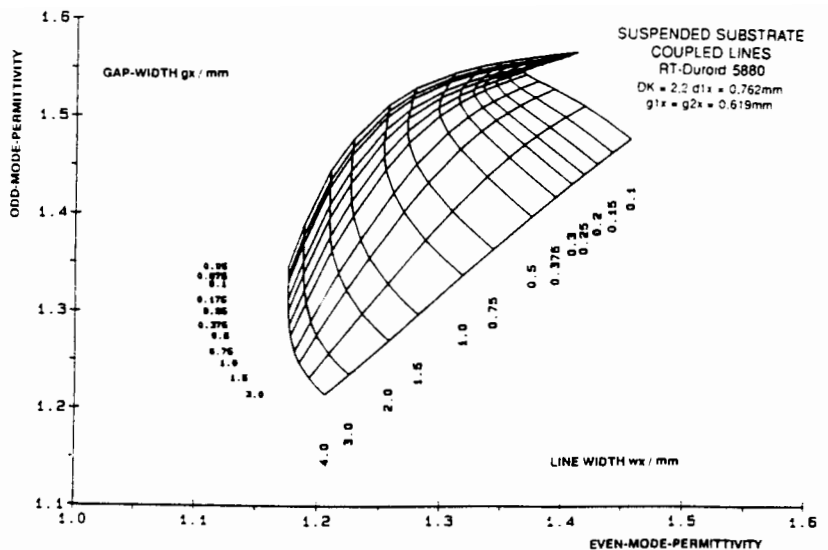


Figure 16. Even- and odd-mode permittivities of suspended substrate coupled lines (substrate, RT 5880).

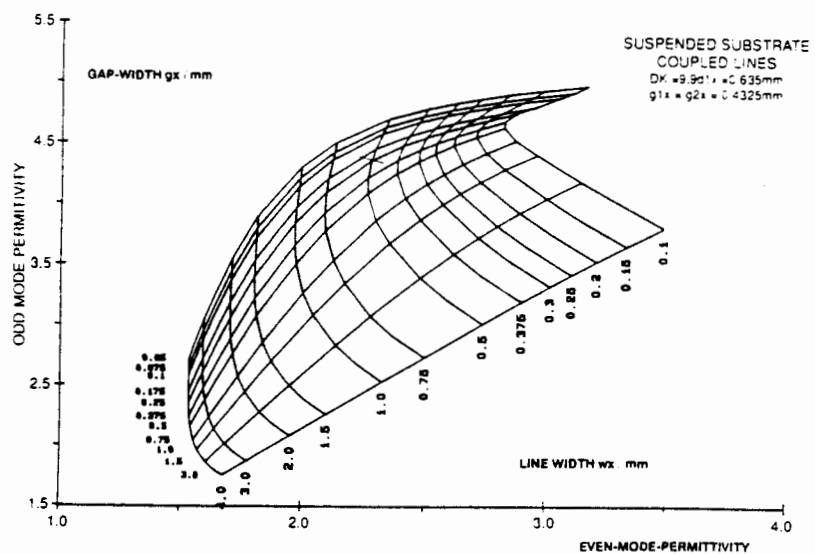


Figure 17. Even- and odd-mode permittivities of suspended substrate coupled lines (substrate, AL 203).

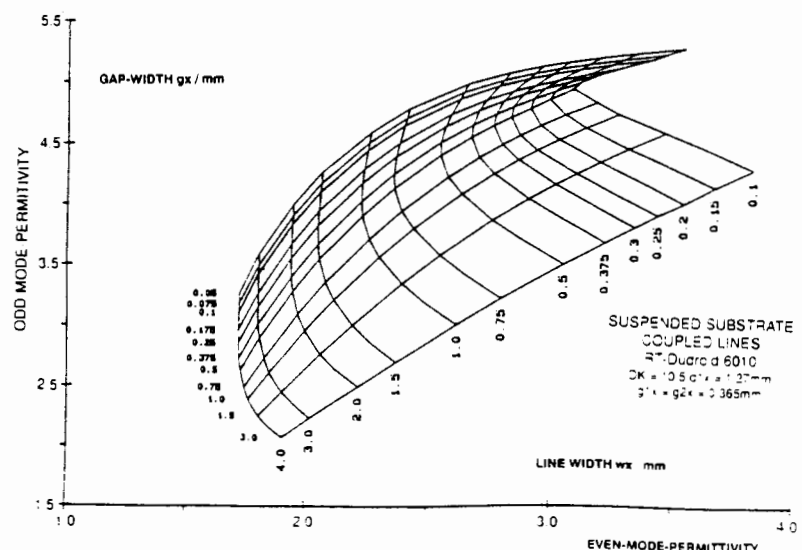
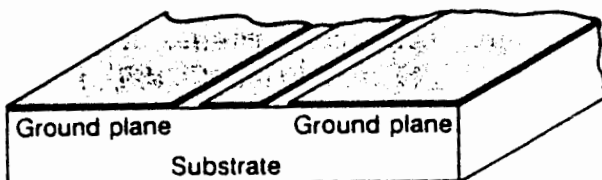
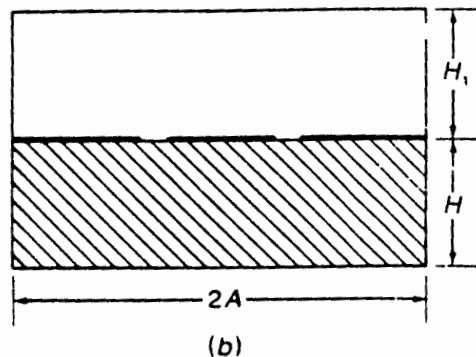
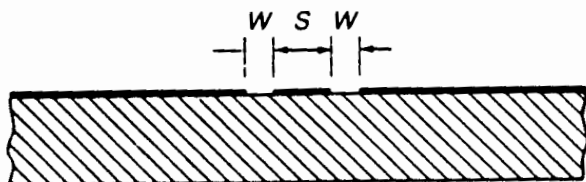
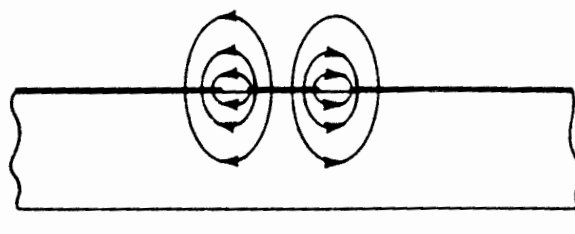


Figure 18. Even- and odd-mode permittivities of suspended substrate coupled lines (substrate, RT 6010).

Ομοενικός Κυματοδοχός (CPW: Coplanar Waveguide)  
 (Collin Eq. 175-)



(a)



(c)

**FIGURE 3.35**

(a) Basic coplanar transmission line; (b) a shielded coplanar transmission line; (c) electric field distribution.

# Ορθογωνικός κυματοδοντός με πάξες.

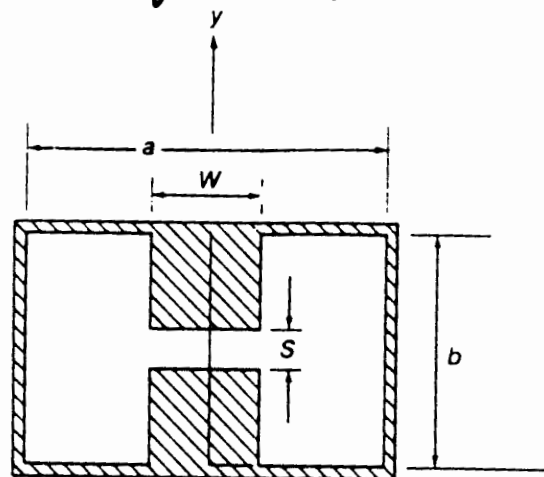


**FIGURE 3.46**  
Ridge waveguide.

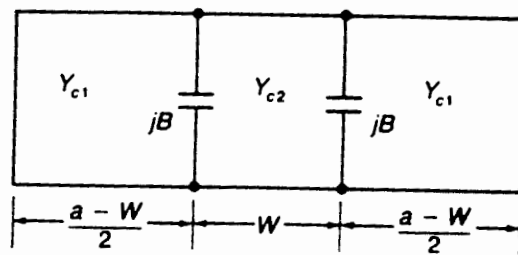


**FIGURE 3.47**  
Equivalent transmission-line circuit of cross section of ridge waveguide.

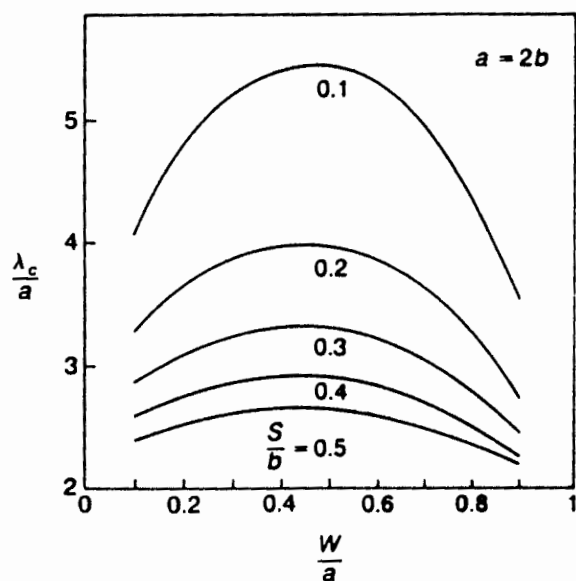


**FIGURE 3.48**  
Normalized cutoff wavelength  $\lambda_c/a$  for a ridge waveguide.

# Τοποδέιν σε Αυτοφοίνιαν Γύρδητην Γε μηχανικά κύκλωμα

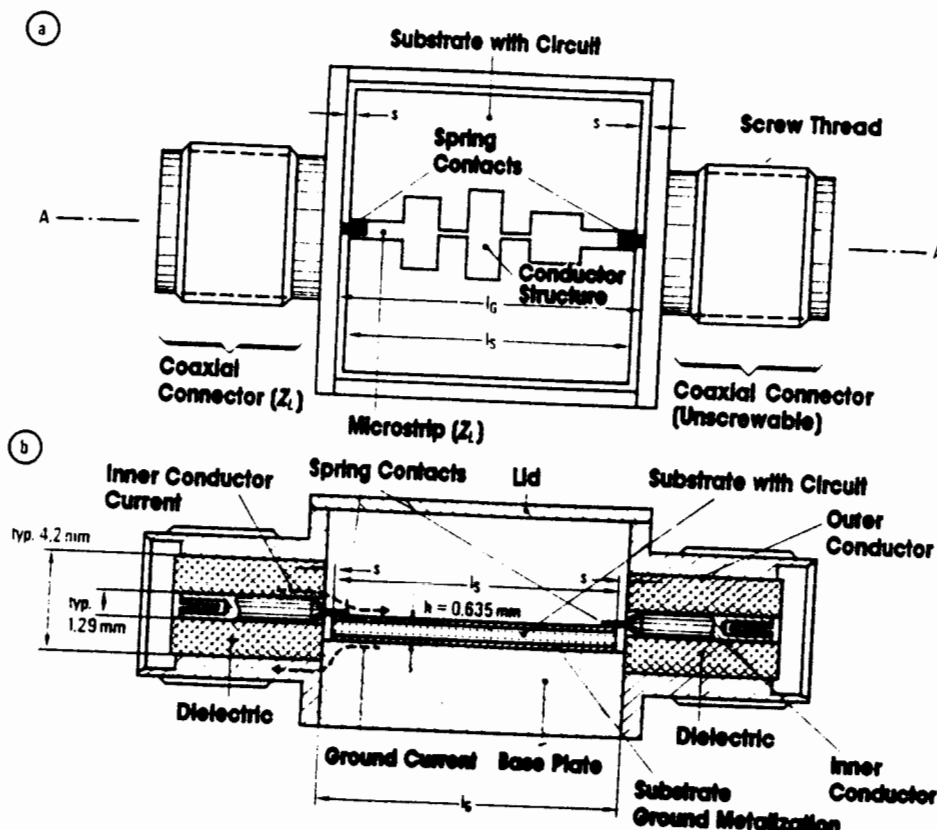
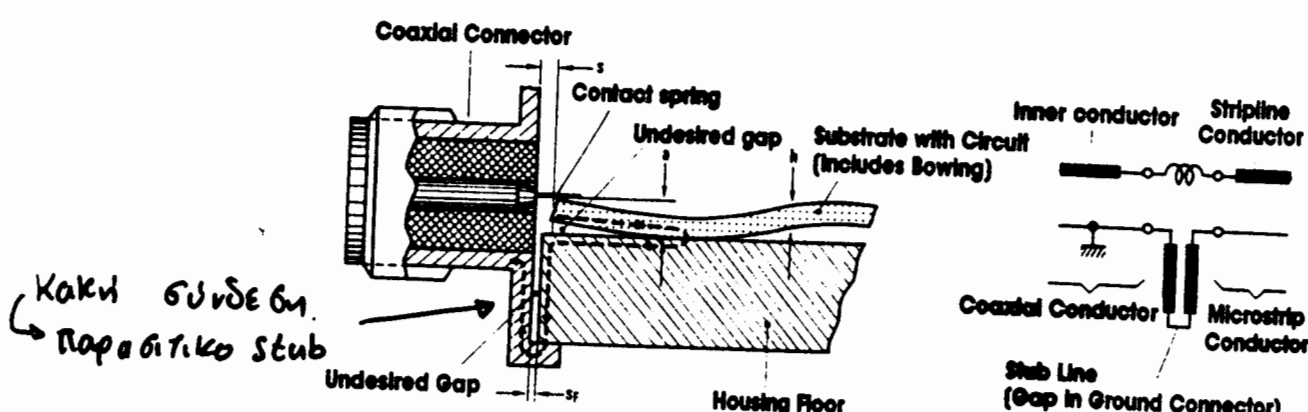


Fig. 1.32 Schematic of a housing for a microstrip circuit with two coaxial connectors: (a) without lid; (b) cross section.

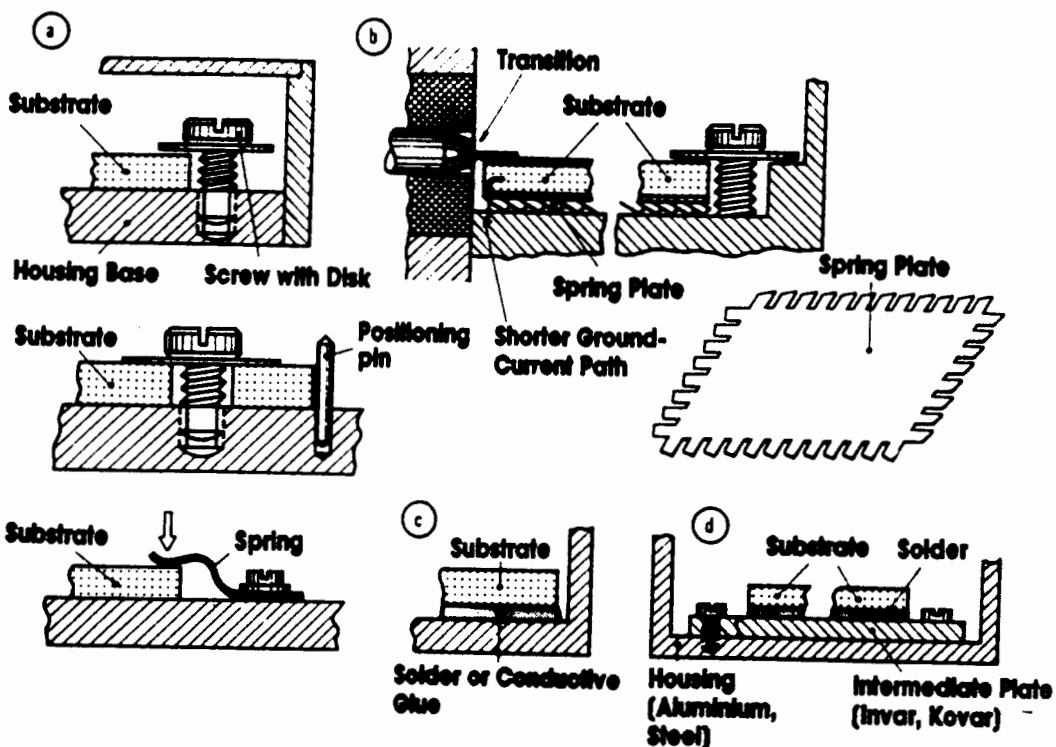
Προβλήμα Διαγράφεων:



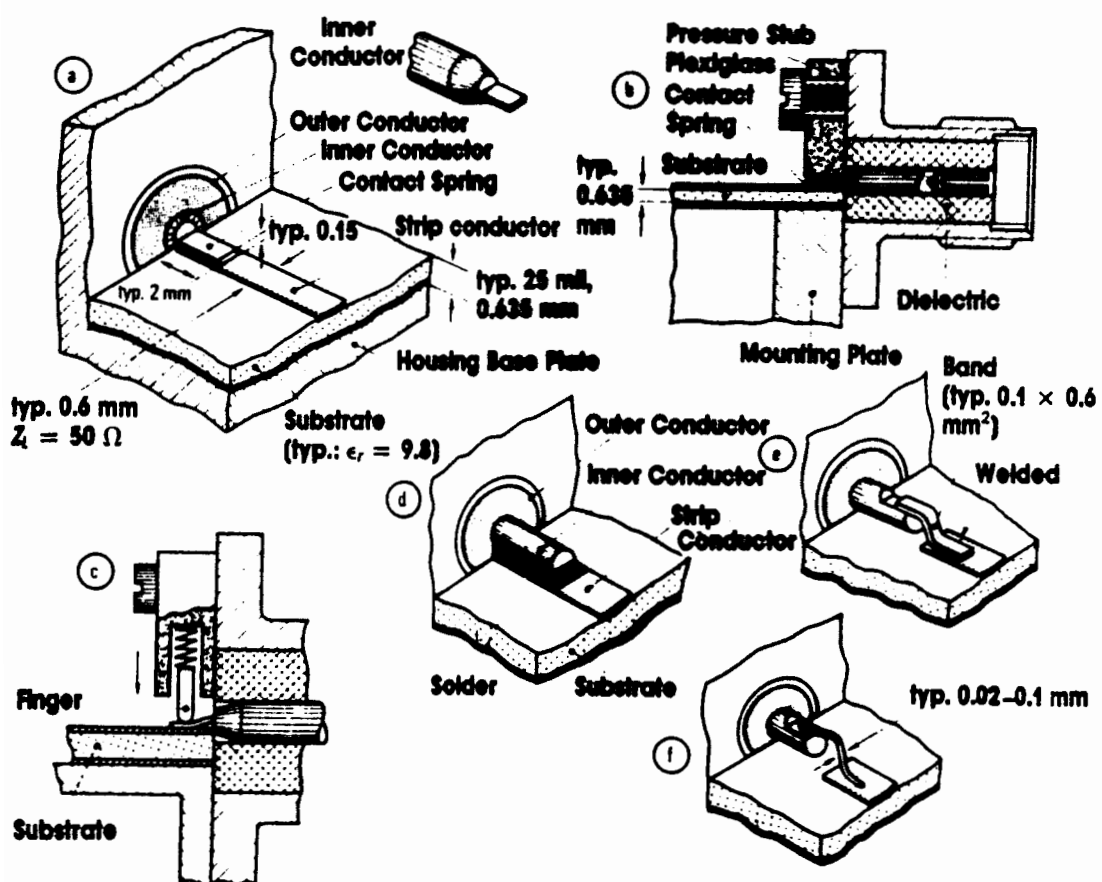
ΠΡΕΓΕΙ:

Fig. 1.33 Action of a bend in the substrate and a split in the ground for a real coaxial-microstrip transition.

- Η αλασματική οι ασυρμόνες των μέσων
- Η αλασματική οι ελασμός διάκοσ πονο πεικάτος
- Η αποθέματα οι διαγραφής γενικές διαστολές



**Fig. 1.34** Possible methods of mounting substrate in housing: (a) clamping; (b) clamping with spring plate; (c) soldering or gluing with conductive paste; (d) soldering onto an intermediate invar plate.



**Fig. 1.35** Possibilities for inner-conductor connectors: (a) gluing with spring ( $f \leq 18$  GHz); (b) as in (a), but with plastic pressure stub; (c) as in (a), but with spring-loaded finger; (d) soldered inner conductor ( $f \leq 1$  GHz); (e) welded strip ( $f \leq 0.5$  GHz); (f) welded wire ( $f \leq 0.2$  GHz).

# Δια 6ερδες Ομοαντλεσί (και μηπο τανταλεύς γεμάτων)

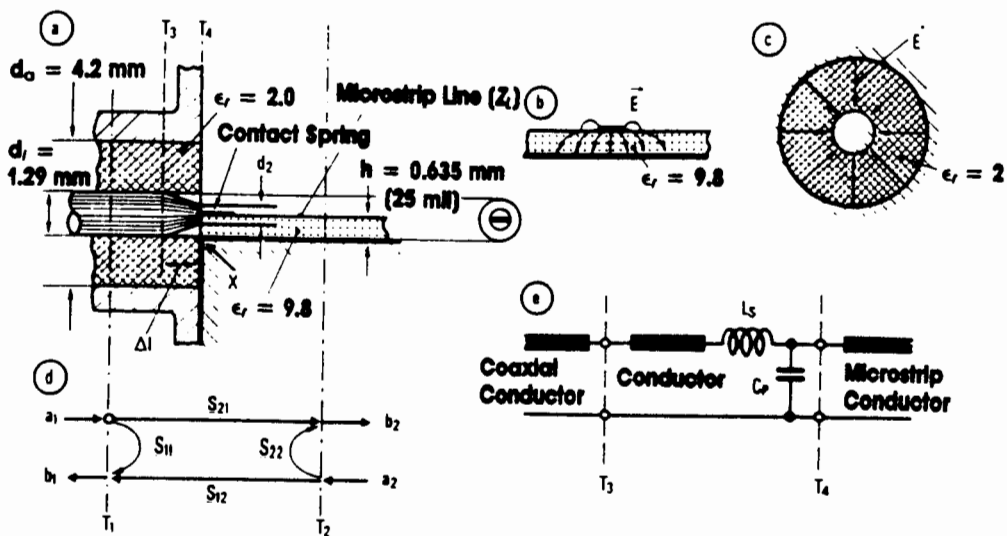


**Fig. 1.37** Transition from SMA-coaxial line to microstrip line, electrical properties: (a) cross section; (b) electrical field pattern of microstrip line; (c) field pattern of coaxial line; (d) general scattering coefficients  $S_{ij}$  of a transition; (e) equivalent circuit of a compensated transition as shown in (a).

Δια 6ερδες

Χαλαρώνεται

α παντείων

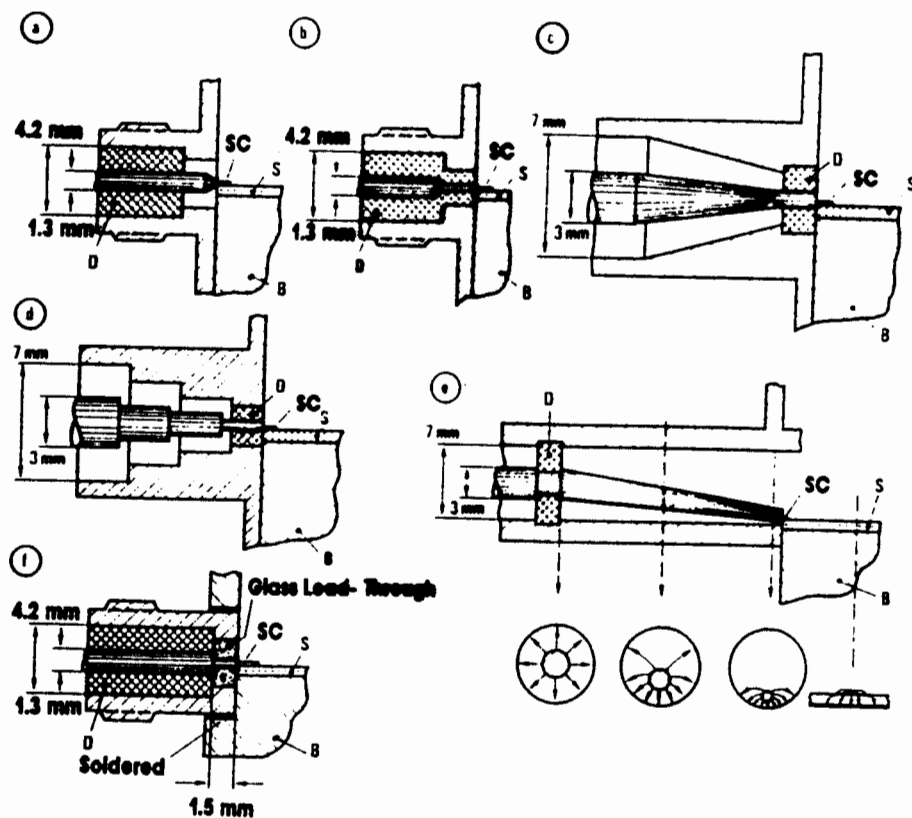


**Fig. 1.38** Other types of low-reflection transitions from 3/7 coaxial line ( $d_{in} = 3 \text{ mm}$ ,  $d_{out} = 7 \text{ mm}$ ) or SMA coaxial line ( $d_{in} = 1.3 \text{ mm}$ ,  $d_{out} = 4.2 \text{ mm}$ ) to microstrip line on ceramic substrate, S (thickness 25 mil =  $0.635 \text{ mm}$ ,  $\epsilon_r = 9.8$ ); SC = inner conductor spring contact; B = housing base plate: (a) with intermediate air conductor; (b) with stepped cross-section matching sections; (c) with continuous cross-section matching; (d) multisteped; (e) eccentric coaxial transition (after [1.319]); (f) hermetically sealed (D = dielectric).

# Δια6ύδε6η αρχή γνώσης κυπετοδημα - Mikrotalviallio Spafis

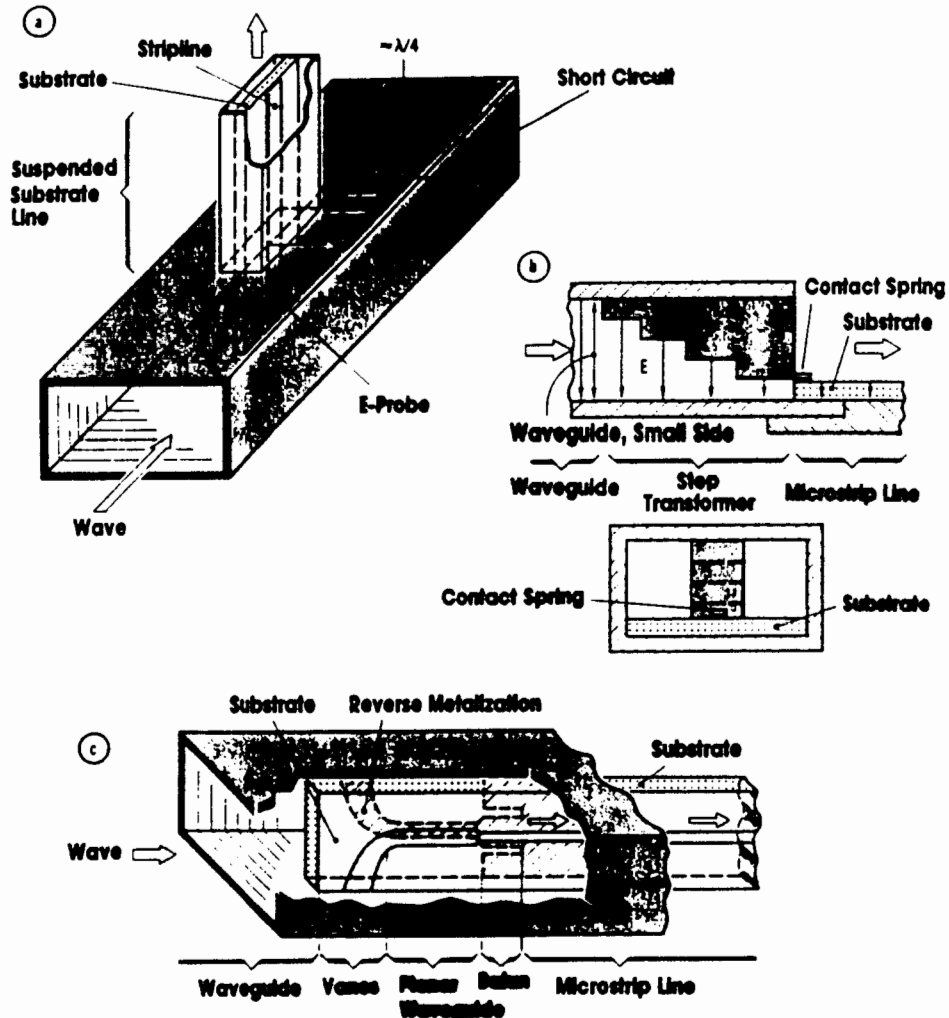


**Fig. 1.40** Transitions from rectangular waveguide to stripline conductors:  
 (a) E-field probe coupling via suspended-substrate line (after [1.347]); (b) step-transformer transition to microstrip line (after [1.30]); (c) transition to microstrip line (after [1.329, 1.330]).

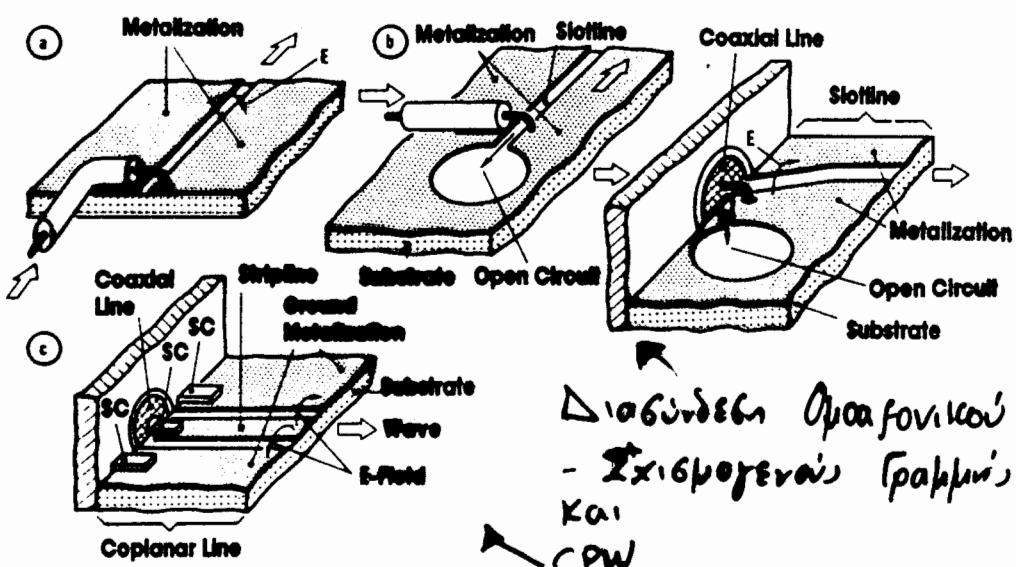


**Fig. 1.41** Transitions from coaxial to slotline and coplanar line: (a) slotline transition at substrate edge [1.349, 1.350]; (b) slotline transition with open circuit [1.351]; (c) coplanar line transition (SC = spring contacts for inner conductor and grounds).